

# Contextual Scenario Generation for Two-Stage Stochastic Programming

David Islip<sup>1</sup>, Roy H. Kwon<sup>1\*</sup>, Sanghyeon Bae<sup>2</sup>, Woo Chang Kim<sup>2</sup>

<sup>1</sup>Department of Mechanical and Industrial Engineering, University of Toronto, 5 King's College Rd, Toronto, M5S 3G8, Ontario, Canada.

<sup>2</sup>Department of Industrial and Systems Engineering, Korea Advanced Institute of Science and Technology (KAIST), 291 Daehak-ro, Yuseong-gu, Daejeon, 34141, Republic of Korea.

\*Corresponding author(s). E-mail(s): [rkwon@mie.utoronto.ca](mailto:rkwon@mie.utoronto.ca) .

Contributing authors: [ryan.islip@mail.utoronto.ca](mailto:ryan.islip@mail.utoronto.ca) .

[azureharry@kaist.ac.kr](mailto:azureharry@kaist.ac.kr) ; [wkim@kaist.ac.kr](mailto:wkim@kaist.ac.kr) .

## Abstract

Two-stage stochastic programs (2SPs) are important tools for making decisions under uncertainty. Decision-makers use contextual information to generate a set of scenarios to represent the true conditional distribution. However, the number of scenarios required is a barrier to implementing 2SPs, motivating the problem of generating a small set of surrogate scenarios that yield high-quality decisions when they represent uncertainty. Current scenario generation approaches do not leverage contextual information or do not address computational concerns. In response, we propose contextual scenario generation (CSG) to learn a mapping between the context and a set of surrogate scenarios of user-specified size. First, we propose a distributional approach that learns the mapping by minimizing a distributional distance between the predicted surrogate scenarios and the true contextual distribution. Second, we propose a task-based approach that aims to produce surrogate scenarios that yield high-quality decisions. The task-based approach uses neural architectures to approximate the downstream objective and leverages the approximation to search for the mapping. The proposed approaches apply to various problem structures and loosely only require efficient solving of the associated subproblems and 2SPs defined on the reduced scenario sets. Numerical experiments demonstrating the effectiveness of the proposed methods are presented.

**Keywords:** Stochastic Programming, Scenario Generation, End-to-end learning, Contextual Optimization

# 1 Introduction

Two-stage stochastic programming is a widely adopted decision modeling approach that enables decision-makers to account for uncertainty that unfolds over two stages. The structure is as follows: decisions are made in the first stage before some uncertainty is realized, after which the decision maker has recourse and responds to the realized uncertainty (second stage). There is a cost for the first-stage decision, and for each specific realization of uncertainty, there is a cost linked to the recourse actions. Consequently, a common objective is to minimize the combined cost of the first-stage decision and the expected cost of recourse actions. Ntairo [1] provides a recent survey of various applications of two-stage stochastic programming in logistics, portfolio management, and manufacturing, among others.

In the two-stage setting, the decision maker selects a first-stage decision  $\mathbf{y}$  by solving a two-stage stochastic program (2SP)

$$\min_{\mathbf{y}} h(\mathbf{y}) + \mathbb{Q}(\mathbf{y}) \quad \text{s.t.} \quad \mathbf{y} \in \mathcal{Y}, \quad \mathbf{y} \in \mathbb{R}^{s_1}, \quad (2SP)$$

where  $h : \text{dom}(h) (\subseteq \mathbb{R}^{s_1}) \rightarrow \text{codom}(h) (\subseteq \mathbb{R})$  models the cost of the first-stage decision, with  $\text{dom}(h)$  and  $\text{codom}(h)$  denoting the domain and codomain of  $h$  respectively. Additionally,  $\mathcal{Y}$  is the feasible set for first-stage decisions,  $\omega \in \Omega \subseteq \mathbb{R}^p$  represents the uncertainty distributed according to the probability measure  $\mathbb{P}$ , and  $\mathbb{Q}(\mathbf{y}) = \mathbb{E}_{\mathbb{P}}[Q(\mathbf{y}, \omega)]$  is the expected recourse cost with  $Q(\mathbf{y}, \omega)$  denoting the recourse cost of the first-stage decision  $\mathbf{y}$  when uncertainty  $\omega$  is realized. After the first-stage decision is made and uncertainty is realized, the decision maker has recourse  $\mathbf{z}$  and determines the best recourse action by minimizing the cost

$$Q(\mathbf{y}, \omega) = \min_{\mathbf{z}} q(\mathbf{z}, \omega) \quad \text{s.t.} \quad \mathbf{z} \in \mathcal{Z}(\mathbf{y}, \omega), \quad \mathbf{z} \in \mathbb{R}^{s_2}, \quad (\text{Stage II})$$

where  $q : \text{dom}(q) (\subseteq \mathbb{R}^{s_2} \times \mathbb{R}^p) \rightarrow \text{codom}(q) (\subseteq \mathbb{R})$  models the recourse cost for uncertainty  $\omega \in \Omega \subseteq \mathbb{R}^p$ , the feasible set of recourse actions given the first-stage decision  $\mathbf{y}$  and uncertainty  $\omega$  is denoted by  $\mathcal{Z}(\mathbf{y}, \omega)$ . The following assumption is often employed for 2SPs, and we adopt it also.

**Assumption 1.** *It is assumed that (Stage II) can be solved efficiently.*

Solving (2SP) involves evaluating a multidimensional integral that is usually not analytically tractable or amenable to numerical integration due to high dimensionality. Thus, the distribution is often represented by a finite set of scenarios  $\hat{\Omega} = \{\omega^{(j)}\}_{j=1}^M \subseteq \Omega$ . Sample average approximation (SAA) is a common approach for generating scenarios, which proceeds by sampling  $\hat{\Omega}$  from  $\mathbb{P}$  [2]. Using  $\hat{\Omega}$ , the following problem is then solved in place of (2SP)

$$\min_{\mathbf{y} \in \mathcal{Y} \cap \mathbb{R}^{s_1}} h(\mathbf{y}) + \frac{1}{|\hat{\Omega}|} \sum_{j=1}^{|\hat{\Omega}|} \min_{\mathbf{z} \in \mathcal{Z}(\mathbf{y}, \omega^{(j)})} q(\mathbf{z}, \omega^{(j)}). \quad (2SP\text{-SAA})$$

Although SAA is asymptotically optimal, solving (2SP-SAA) on a small sample of scenarios can lead to suboptimal first-stage decisions and large sample sets are required

to obtain high-quality solutions. One possible approach to solve (2SP-SAA) is to solve the *extensive form*; a deterministic program formed by introducing scenario-specific copies of the second-stage variables. The size of the extensive form grows linearly with  $M$ , necessitating algorithms tailored to specific problem classes. Unfortunately, it is widely accepted that optimally solving (2SP-SAA) is intractable due to complicating problem components such as non-linear objectives and integrality requirements [3, 4]. Hence, the distribution is often represented by a small set of scenarios consisting of a positive integer  $K$  number of scenarios, referred to as surrogate scenarios  $\zeta_{1\dots K} \in \Omega^K$ , with the following implicit assumption.

**Assumption 2.** (2SP-SAA) can be efficiently solved on  $K$  scenarios for sufficiently small values of  $K$ .

Ideally,  $\zeta_{1\dots K}$  are selected to ensure that the solution to (2SP-SAA) on the reduced set is nearly optimal with respect to the (2SP) objective under  $\mathbb{P}$ . This process is known as *scenario generation*. Typically, scenario generation is done by generating a discretized representation of  $\mathbb{P}$  or by sampling a large number of scenarios  $\hat{\Omega}$  from  $\mathbb{P}$  and performing *scenario reduction* to reduce its size from  $M$  to  $K$  with  $K \ll M$ . Scenario generation encapsulates either case.

In practice, decision-makers are often tasked with making decisions repeatedly in different settings. Often, decision-makers find themselves in a contextual setting where they are faced with (i) a decision-making problem endowed with uncertainty  $\omega$  that impacts the problem’s important elements and (ii) the opportunity to exploit side-information that is correlated with  $\omega$  at decision-making time. This work focuses on decision-making via 2SPs in a contextual setting. The side information, also referred to as contextual information  $\mathbf{x} \in \mathcal{X} \subseteq \mathbb{R}^d$ , follows a joint distribution with  $\omega$  denoted by  $\mathbb{P}_{(\mathbf{x}, \omega)}$ . The marginal distribution of  $\mathbf{x}$  and the conditional distribution of  $\omega$  given  $\mathbf{x}$  are denoted by  $\mathbb{P}_{\mathbf{x}}$  and  $\mathbb{P}_{\omega|\mathbf{x}}$  respectively. A realization of the context  $\hat{\mathbf{x}}$  is observed before the first-stage decision, and as such, the decision maker wishes to solve (2SP) with expected costs evaluated over  $\mathbb{P}_{\omega|\mathbf{x}=\hat{\mathbf{x}}}$ . We consider the following example to motivate the contextual setting.

**A Motivating Example:** Higle and Sen [5] introduce CEP1, a two-stage machine capacity expansion problem for a flexible manufacturing facility. The decision maker must plan the expansion of production capacity for  $m$  parts on  $n_{\text{machines}}$  machines. In its baseline state, machine  $j \in [n_{\text{machines}}] := [1, 2, \dots, n_{\text{machines}}]$  is available for  $h_j$  hours per week, with additional hours available at a cost of  $c_j$  per hour. Machines have usage limits and require maintenance based on usage. Part type  $i \in [m]$  can be produced on machine  $j$  at a rate of  $a_{ij}$  with cost  $g_{ij}$  per hour. The demand  $\omega_i$  for product type  $i$  is uncertain. First, the decision maker determines machine capacities (first stage) and then creates a production plan to minimize costs after demand  $\omega_i$  is realized (second stage). Unmet demand is subcontracted at a premium. In the original problem, capacity decisions are made weekly, but if product demand fluctuates more frequently, adjusting capacity more often (e.g., minutely) may be valuable. This situation could arise if the product demands come from a manufacturing line with variable product demand. Here, context  $\mathbf{x}$  includes data from the assembly line, such as past demands. Capacity decisions must be made quickly while incorporating the uncertain demand, its relationship to the known context, and the available recourse.

**Fig. 1** Optimization with Scenario Generation



*Note.* A standard contextual 2SP approach: (i) estimates the conditional distribution from the data, (ii) generates scenarios via sampling from the estimated distribution, (iii) reduces generated scenarios, and (iv) optimizes based on the reduced set of scenarios

Thus, it is desirable to obtain an approach for efficiently solving 2SPs, repeatedly in different contexts  $\mathbf{x}$ , such that the resulting solution performs well according to the 2SP objective, evaluated according to  $\mathbb{P}_{\omega|\mathbf{x}}$ . However, decision-makers typically do not have access to the conditional distribution and instead only have access to historical data, motivating the following assumption.

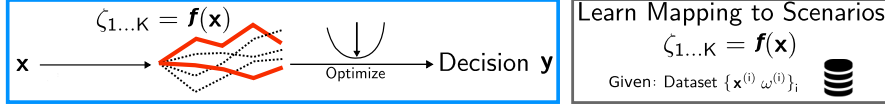
**Assumption 3.** *The decision-maker does not have access to  $\mathbb{P}_{\omega|\mathbf{x}=\hat{\mathbf{x}}}$  and only has access to an independent and identically distributed (iid) sample of  $n$  observations from  $\mathbb{P}_{(\mathbf{x},\omega)}$ , denoted by  $S = \{(\mathbf{x}^{(i)}, \omega^{(i)})\}_{i=1}^n \stackrel{iid}{\sim} \mathbb{P}_{(\mathbf{x},\omega)}$ .*

It is sensible for the decision maker to use  $S$  to estimate  $\mathbb{P}_{\omega|\mathbf{x}}$ , denoted by  $p_{\theta}(\omega|\mathbf{x})$  and parameterized by  $\theta$ . Figure 1 outlines a traditional approach to contextual 2SP based on the abovementioned considerations. First, data is used to estimate  $p_{\theta}(\omega|\mathbf{x})$ . A realization of the context  $\hat{\mathbf{x}}$  is observed. However, solving (2SP) with the estimated conditional distribution is not analytically tractable, thus, SAA is employed and a set of samples is generated via  $p_{\theta}(\omega|\mathbf{x} = \hat{\mathbf{x}})$ . The resulting instance of (2SP-SAA) is often unwieldy, and the scenarios are reduced to the set of surrogate scenarios  $\zeta_{1...K}$  using a scenario reduction approach. The resulting instance of (2SP-SAA) is finally solved on the reduced set of scenarios, yielding a first-stage solution. The combination of sampling from the estimated conditional distribution and the subsequent scenario reduction constitutes the standard approach one would take to generate  $K$  scenarios in a contextual setting. Figure 1 visually outlines this approach.

A downside of the approach in Figure 1 occurs when the decision maker is faced with a context realization  $\hat{\mathbf{x}}$  since the scenarios must be sampled from  $p_{\theta}(\omega|\mathbf{x})$  and subsequently reduced. Generally, scenario reduction algorithms have computational cost that scales at least linearly in the number of sampled scenarios. The justification of this claim is contained in the overview of scenario generation methods.

In time-sensitive applications where solutions to (2SP) are desired under different contexts, a mapping  $\mathbf{f} : \mathbf{x} \mapsto \zeta_{1...K}$ , that is cheaply evaluated is desirable so that one obtains first-stage decisions in a short amount of time. This process of mapping context to surrogate scenarios and ultimately to a decision is referred to as *Contextual Scenario Generation (CSG)* and forms the base of the methodology proposed in this work. The mapping  $\mathbf{f}$  is called the task-mapping. Ultimately, the success of CSG rests on the ability to select  $\mathbf{f}$ , such that solving (2SP-SAA) on the resulting scenarios yields high-quality decisions. The ultimate goal of this work is to develop a general methodology for constructing a high-quality  $\mathbf{f}$  for general 2SPs, given that we have access to historical data. The proposed CSG approach is shown visually in Figure 2.

**Fig. 2** Contextual Scenario Generation and Optimization



*Note.* Contextual Scenario Generation and Optimization: (i) aims to learn a mapping  $\mathbf{f}$  from data such that  $\mathbf{f} : \mathbf{x} \mapsto \zeta_{1...K}$ , (ii) the predicted scenarios  $\mathbf{f}$  are close in distributional distance to  $\mathbb{P}_{\omega|\mathbf{x}}$ , and (iii) solving 2SP on  $\mathbf{f}$  yields high-quality solutions according to the 2SP objective evaluated using  $\mathbb{P}_{\omega|\mathbf{x}}$ .

## Contributions

The main contributions of this work are as follows:

- This work presents the first framework for solving two-stage stochastic programs in a contextual setting by learning a mapping to a set of surrogate scenarios from the context available to the decision maker. We propose a distributional approach that aims to produce surrogate scenarios that mimic the true conditional distribution, followed by a problem-driven approach that considers the cost of the first-stage solution obtained via solving 2SP-SAA on the surrogate scenarios.
- The proposed methodology makes minimal assumptions about the structure of the 2SP and loosely only requires Assumptions 1-3.
- Computational experiments are performed using four application problems to demonstrate the proposed methodology's ability to produce high-quality solutions in various application domains with differing problem structures. We illustrate the proposed approach using the newsvendor problem, CEP1, portfolio optimization, and a multidimensional newsvendor problem with customer-directed substitutions.

## Structure of the paper

First, Section 2 provides background on scenario generation in stochastic programming, learning-based approaches and their use in stochastic programming, and an overview of solving difficult optimization problems via surrogate optimization. Section 3 introduces the proposed distributional and problem driven approaches. Section 4 presents the experimental setup and results of the computational experiments. Lastly, Section 5 summarizes the results, contributions, and concludes.

## 2 Related Works

### 2.1 Contextual Optimization for Stochastic Programming

This section highlights works focused on contextual stochastic optimization that are most related to the proposed methodology. We refer the reader to Sadana et al. [6] for a more general survey. Furthermore, we leverage the categorization of contextual stochastic optimization introduced by Estes and Richard [7]. The first general approach, referred to as *conditional-density-estimation-then-optimize* estimates  $\mathbb{P}_{\omega|\mathbf{x}}$  then solves (2SP) with the estimated conditional distribution. For example, in the

case of 2SPs, Ban et al. [8] use residuals from the trained regression models to estimate conditional distributions, whereas Bertsimas and Kallus [9] reweighs samples to approximate  $\mathbb{P}_{\omega|\mathbf{x}}$ . However, as pointed out in the introduction, this typically yields a difficult problem, motivating the generation a manageable number of scenarios.

The second approach referred to as *direct-solution-prediction*, aims to directly estimate a mapping from the context  $\mathbf{x}$  to decisions  $\mathbf{y}$  such that the decisions are of high quality, yielding a policy optimization problem. For example, in the case of 2SPs, Yilmaz and Büyüktaktakın [10] formulate a multiagent actor critique approach to solving contextual two-stage knapsack problems where the agents predict solutions to the first and second stages, respectively. Although the solution-prediction approach is effective in tailored settings, it is difficult to deal with general integrality constraints and other complicating problem features [3, 11].

The *predict-then-optimize* approach generates a point prediction of uncertainty from the context and solves (2SP) using a corresponding singleton distribution. Naive versions use standard loss functions (e.g., least-squares), while *smart predict-then-optimize* selects the predictor based on decision performance. For linear programs, Elmachtoub and Grigas [12] minimize decision regret with a surrogate loss function. Estes and Richard [7] apply similar methods to linear 2SPs. Other approaches update models using gradients of downstream performance [13] but struggle with uninformative gradients [11, 14]. To address this, Zharmagambetov et al. [11] propose modelling a surrogate loss function via neural networks. However, early iterations often lead to predictors whose predictions lie outside the region where the model accurately captures the loss, resulting in what we call *loss error maximization*. Moreover, point predictions implicitly assume perfect knowledge, leading to decisions poorly hedged against uncertainty [15].

The proposed CSG approach aims to address these concerns in the general setting of a large class of 2SPs, circumventing computational concerns by generating a small subset of scenarios and subsequently solving (2SP-SAA). This avoids feasibility issues commonly encountered in the direct-solution-prediction approach. Furthermore, the approach inherits all the problem-class generality of Zharmagambetov et al. [11]’s approach while addressing the issue of loss error maximization. Lastly, CSG produces solutions that hedge against uncertainty by considering the surrogate scenarios as opposed to a single prediction.

## 2.2 Scenario Generation

Scenario generation techniques can be categorized into distributional and problem-based approaches. The distributional approach generates surrogate scenarios to mimic some features of the underlying distribution. This aim is typically achieved by minimizing a distributional distance [16] or by matching moments [17] between the scenarios and the underlying distribution. In contrast, problem-driven scenario generation methods account for problem-specific structures so that the resulting scenarios yield high-quality solutions when evaluated using the underlying distribution. Some problem driven approaches include: clustering scenarios based on objective values of candidate solutions [18], identifying irrelevant scenarios based on the objective [19], and approximating the recourse function of a pool of candidate solutions [20]. In our

setting, the scenario generation methods mentioned assume access to the conditional distribution or a sufficiently accurate scenario representation with enough samples  $M$ . One can estimate the conditional distribution as in the conditional-density-estimation-then-optimize approach; however, the generic problem-driven approaches depend at least linearly on  $M$ . In contrast, besides optimizing implementation error, the proposed CSG approach generates surrogate scenarios via a neural network forward pass, eliminating dependence on  $M$  at decision time.

### 2.3 Learning-based Approaches for Stochastic Programs

Machine learning has been applied to solve stochastic programs by predicting solutions or costs. In particular, approaches that leverage machine learning to predict the recourse cost are most relevant to this work. For example, Patel et al. [3], Lee et al. [21] and Bae et al. [22] predict expected recourse in generic 2SPs, leveraging these predictions in the solution of 2SPs. However, these methods do not directly address scenario generation. Although, some works apply machine learning to scenario generation. Bengio et al. [23] use regression to predict a single representative scenario for 2SP such that the scenario minimizes implementation error, but their method relies on heuristically generated datasets and doesn't handle multiple scenarios. Wu et al. [4] employ semi-supervised learning and conditional variational auto-encoders to generate scenario embeddings that align with the optimal expected cost of 2SP based on a subset of solved instances. Unlike their approach, which doesn't explicitly minimize implementation error, this work does not require the ability to solve large-scale 2SPs and instead assumes the ability to solve 2SPs on up to  $K$  scenarios.

## 3 Proposed Methodology

This section introduces the relevant tools from scenario generation in Section 3.1, followed by the proposed distributional contextual scenario generation approach in Section 3.2. Analogously, Section 3.3 introduces a bi-level approach to scenario generation and discusses its properties, followed by its contextual extension to our setting in Section 3.4 and the associated solution approach in Section 3.5.

### 3.1 Preliminaries: Distributional Scenario Generation

Römisch [24] argue that integral probability metrics (IPMs) are a sensible choice of distances for 2SPs since IPMs such as the Fortet-Mourier and Wasserstein distances lead to stability bounds for 2SPs and form the basis of several existing scenario generation approaches. Given a class of real-valued bounded measurable functions associated with the sample space  $\Omega$  along with two distributions  $\mathbb{P}_\omega$  and  $\mathbb{P}_\eta$  on  $\Omega$ , IPMs take the form

$$d_{\mathcal{G}}(\mathbb{P}_\omega, \mathbb{P}_\eta) = \sup_{g \in \mathcal{G}} |\mathbb{E}_{\omega \sim \mathbb{P}_\omega}[g(\omega)] - \mathbb{E}_{\eta \sim \mathbb{P}_\eta}[g(\eta)]|.$$

Different choices of  $\mathcal{G}$  yield different distances. For example, when  $\mathcal{G}$  is the set of 1-Lipshitz functions,  $d_{\mathcal{G}}(\cdot, \cdot)$  corresponds to the 1-Wasserstein distance. Another metric of interest, maximum mean discrepancy (MMD), corresponds to the class

$\mathcal{G}_{\text{MMD}} = \{g \in \mathcal{H} : \|g\|_\infty \leq 1\}$  where  $\mathcal{H}$  denotes a Reproducing Kernel Hilbert Space (RKHS) with associated positive semi-definite kernel  $k : \Omega \times \Omega \rightarrow \mathbb{R}$ . The kernel mean embedding of  $\mathbb{P}_\omega$  in  $\mathcal{G}_{\text{MMD}}$  is given by  $\mu_{\mathbb{P}_\omega} := \mathbb{E}_{\omega \sim \mathbb{P}_\omega} [k(\cdot, \omega)]$ , and is guaranteed to be an element of  $\mathcal{G}_{\text{MMD}}$  if  $\mathbb{E}_{\omega \sim \mathbb{P}_\omega} [\sqrt{k(\omega, \omega)}] < \infty$ <sup>1</sup> [25]. Gretton et al. [25] showed that the squared MMD is given by

$$\begin{aligned} d_{\mathcal{G}_{\text{MMD}}}^2(\mathbb{P}_\omega, \mathbb{P}_\eta) &= \|\mu_{\mathbb{P}_\omega} - \mu_{\mathbb{P}_\eta}\|_{\mathcal{G}_{\text{MMD}}}^2 \\ &= \mathbb{E}_{(\omega, \omega') \sim \mathbb{P}_\omega} [k(\omega, \omega')] + \mathbb{E}_{(\eta, \eta') \sim \mathbb{P}_\eta} [k(\eta, \eta')] - 2\mathbb{E}_{\omega \sim \mathbb{P}_\omega, \eta \sim \mathbb{P}_\eta} [k(\omega, \eta)], \end{aligned}$$

where  $\|\cdot\|_{\mathcal{G}_{\text{MMD}}}$  denotes the norm in the RKHS  $\mathcal{G}_{\text{MMD}}$ . A kernel  $k$  is characteristic if  $\mu : \mathbb{P} \mapsto \mu_{\mathbb{P}}$  is injective. Characteristic kernels guarantee that  $d_{\mathcal{G}_{\text{MMD}}}^2(\mathbb{P}_\omega, \mathbb{P}_\eta) = 0 \iff \mathbb{P}_\omega = \mathbb{P}_\eta$ . For more details regarding RKHS and embeddings of probability distributions, the reader is referred to [25, 26].

For a given context  $\mathbf{x}$ , the distributional scenario generation (DSG) problem solves

$$\min_{\zeta_1, \dots, \zeta_K} d_{\mathcal{G}}(\mathbb{P}_{\zeta_1 \dots \zeta_K}, \mathbb{P}_{\omega|\mathbf{x}}), \quad (\text{DSG})$$

where  $\mathbb{P}_{\zeta_1 \dots \zeta_K} = \frac{1}{K} \sum_{k=1}^K \delta_{\zeta_k}$  is the empirical measure associated with the scenarios  $\zeta_1 \dots \zeta_K$  and  $\delta_\zeta$  is the Dirac delta function centered at  $\zeta$ . However, as pointed out in the introduction, in practice one only has historical data  $S$  that is used to form an estimate  $p_\theta(\omega|\mathbf{x})$  of  $\mathbb{P}_{\omega|\mathbf{x}}$ . In response, a sufficiently large number of samples are sampled from  $p_\theta(\omega|\mathbf{x})$  and (DSG) is solved with  $\mathbb{P}_{\omega|\mathbf{x}}$  replaced with the empirical measure supported on the samples. The next section presents the proposed contextual extension of (DSG).

### 3.2 Distributional Contextual Scenario Generation

Given a contextual realization  $\hat{\mathbf{x}}$ , the decision maker wishes to use  $\mathbb{P}_{\omega|\mathbf{x}=\hat{\mathbf{x}}}$  to evaluate the expectation in (2SP). We propose selecting  $\mathbf{f} : \mathbf{x} \mapsto \zeta_1 \dots \zeta_K$  from a vector-valued function class  $\mathcal{F}$  such that the distributional distance between the empirical distribution supported on  $\mathbf{f}(\mathbf{x})$  and  $\mathbb{P}_{\omega|\mathbf{x}}$  is minimized in expectation over  $\mathbb{P}_{\mathbf{x}}$ . We refer to  $\mathcal{F}$  as the hypothesis set for the task-mapping. This approach is referred to as distributional contextual scenario generation (DCSG)

$$\min_{\mathbf{f} \in \mathcal{F}} \mathcal{L}_{\text{dist}}(\mathbf{f}) := \mathbb{E}_{\mathbf{x} \sim \mathbb{P}_{\mathbf{x}}} [d(\mathbb{P}_{\mathbf{f}(\mathbf{x})}, \mathbb{P}_{\omega|\mathbf{x}})], \quad (\text{DCSG})$$

where  $\mathbb{P}_{\mathbf{f}(\mathbf{x})} = \frac{1}{K} \sum_{k=1}^K \delta_{f_k(\mathbf{x})}$  is the empirical measure associated with the scenarios  $\mathbf{f}(\mathbf{x})$  and  $d(\cdot, \cdot)$  is a measure of distance between the distributions. It is not clear what class of distances should be used in the contextual setting. Several authors have considered this question in the context of generative modeling using both Wasserstein and MMD distances. A more thorough comparison of the different approaches to comparing conditional distributions is provided in Appendix A. Huang et al. [27]'s work is similar to ours as they consider the same objective but in the setting of

---

<sup>1</sup>This technical assumption is not overly restrictive since it holds for continuous kernels on compact domains or continuous bounded kernels.



generative models. In this work, we set  $d = d_{\mathcal{G}_{\text{MMD}}}^2$  due to the desirable properties it affords  $\mathcal{L}_{\text{dist}}$  in the proposed contextual setting, which we discuss next.

First, Huang et al. [27] provide the following theorem, showing that  $\mathcal{L}_{\text{dist}}(\mathbf{f})$  is a metric.

**Theorem 1** (Theorem 4, from [27]). *If (i)  $k(\cdot, \cdot)$  is characteristic and measurable, (ii)  $\mathbb{E}_{\omega \sim \mathbb{P}_{\omega|\mathbf{x}}} [k(\omega, \omega)] < \infty$  and (iii)  $\mathbb{E}_{\omega \sim \mathbb{P}_{\mathbf{f}(\mathbf{x})}} [k(\omega, \omega)] < \infty$  for all  $\mathbf{x} \in \mathcal{X}$ , then  $\mathcal{L}_{\text{dist}}(\mathbf{f}) \geq 0$  and  $\mathcal{L}_{\text{dist}}(\mathbf{f}) = 0 \iff \mathbb{P}_{\mathbf{f}(\mathbf{x})} = \mathbb{P}_{\omega|\mathbf{x}}$  almost everywhere according to  $\mathbb{P}_{\mathbf{x}}$ .*

Next, we note that  $\mathcal{L}_{\text{dist}}(\mathbf{f})$  can be optimized over  $\mathbf{f}$  using only joint samples.  $\mathcal{L}_{\text{dist}}(\mathbf{f})$  can be written as

$$\begin{aligned} \mathcal{L}_{\text{dist}}(\mathbf{f}) &= \mathbb{E}_{\mathbf{x} \sim \mathbb{P}_{\mathbf{x}}} \left[ \mathbb{E}_{(\omega, \omega') \sim \mathbb{P}_{\omega|\mathbf{x}}} [k(\omega, \omega')] + \frac{1}{K^2} \sum_{i=1}^K \sum_{i'=1}^K k(f_i(\mathbf{x}), f_{i'}(\mathbf{x})) \right. \\ &\quad \left. - \frac{2}{K} \sum_{i=1}^K \mathbb{E}_{\omega \sim \mathbb{P}_{\omega|\mathbf{x}}} [k(\omega, f_i(\mathbf{x}))] \right] \\ &= C + \frac{1}{K^2} \sum_{i=1}^K \sum_{i'=1}^K \mathbb{E}_{\mathbf{x} \sim \mathbb{P}_{\mathbf{x}}} [k(f_i(\mathbf{x}), f_{i'}(\mathbf{x}))] \\ &\quad - \frac{2}{K} \sum_{i=1}^K \mathbb{E}_{\mathbf{x} \sim \mathbb{P}_{\mathbf{x}}} \mathbb{E}_{\omega \sim \mathbb{P}_{\omega|\mathbf{x}}} [k(\omega, f_i(\mathbf{x}))] \\ &= C + \underbrace{\mathbb{E}_{(\mathbf{x}, \omega) \sim \mathbb{P}_{\mathbf{x}, \omega}} \left[ \frac{1}{K^2} \sum_{i=1}^K \sum_{i'=1}^K k(f_i(\mathbf{x}), f_{i'}(\mathbf{x})) - \frac{2}{K} \sum_{i=1}^K k(\omega, f_i(\mathbf{x})) \right]}_{:= \ell_{\text{MMD}}(\mathbf{f}(\mathbf{x}), \omega)}, \end{aligned}$$

where  $C = \mathbb{E}_{\mathbf{x} \sim \mathbb{P}_{\mathbf{x}}} \mathbb{E}_{(\omega, \omega') \sim \mathbb{P}_{\omega|\mathbf{x}}} [k(\omega, \omega')]$  is a constant with respect to  $\mathbf{f}$ . Huang et al. [27] point out that evaluating  $C$ , requires  $\omega$  and  $\omega'$  to be drawn in a conditionally independent manner for each  $\mathbf{x}$ , which is not equivalent to globally sampling  $(\mathbf{x}, \omega, \omega')$ , since the latter is not necessarily conditionally independent. Let  $\mathcal{L}_{\text{MMD}}(\mathbf{f}) := \mathbb{E}_{(\mathbf{x}, \omega)} [\ell_{\text{MMD}}(\mathbf{f}(\mathbf{x}), \omega)]$  denote the part of  $\mathcal{L}_{\text{dist}}(\mathbf{f})$  that depends on  $\mathbf{f}$ .

Since  $C$  does not depend on  $\mathbf{f}$ , optimizing  $\mathcal{L}_{\text{MMD}}(\cdot)$  is equivalent to optimizing  $\mathcal{L}_{\text{dist}}(\cdot)$  over  $\mathbf{f}$ . Let  $\hat{\mathcal{L}}_{\text{MMD}}(\mathbf{f}) := \frac{1}{n} \sum_{i=1}^n \ell_{\text{MMD}}(\mathbf{f}(\mathbf{x}^{(i)}), \omega^{(i)})$  denote the sample estimate. In practice, one selects  $\mathbf{f}$  via empirical loss minimization  $\min_{\mathbf{f} \in \mathcal{F}} \hat{\mathcal{L}}_{\text{MMD}}(\mathbf{f})$ . Although  $\hat{\mathcal{L}}_{\text{MMD}}(\cdot)$  is non-convex in general and optimization cannot be performed analytically. In the naive implementation, the computational cost to evaluate the batch gradient over  $S$  is  $K^2 + nK$  kernel evaluations, making optimization computationally tractable for small  $K$ .

In this work, we consider kernel  $k_E(\omega, \omega') = \frac{1}{2} (\|\omega\|_2 + \|\omega'\|_2 - \|\omega - \omega'\|)$  corresponding to the energy-distance [28]. Séjourné et al. [29] point out that optimization over MMD distances induced by parameterized kernels (e.g., the Gaussian kernel) are sensitive to their parameters, making the parameter-free  $k_E$  an attractive choice. Furthermore, one can observe that  $d_{\text{MMD}}^2$  with kernel  $k_E$  is equivalent to selecting the negative Euclidean kernel  $\tilde{k}_E(\omega, \omega') = -\|\omega - \omega'\|_2$ . In this case,  $d_{\text{MMD}}^2$  respects the

underlying geometry via scale equivariance [30]. That is, for  $d_{\mathcal{G}_{\text{MMD}}}^2(\mathbb{P}_\omega, \mathbb{P}_\eta)$ , scaling the sample spaces of  $\mathbb{P}_\omega$  and  $\mathbb{P}_\eta$  by  $c \in \mathbb{R}$ , scales  $d_{\mathcal{G}_{\text{MMD}}}^2(\mathbb{P}_\omega, \mathbb{P}_\eta)$  by  $|c|$ . Furthermore, it is interesting to note that, in the case of the energy kernel  $\tilde{k}_E$ , along with setting  $K = 1$ , optimizing  $\mathcal{L}_{\text{MMD}}(\mathbf{f})$  reduces to least-squares.

The energy distance satisfies the assumptions in Theorem 1. Assumptions (ii) and (iii) in Theorem 1, reduce to the bounded moment conditions present in Proposition 1 by Székely and Rizzo [30]. Proposition 1 by Székely and Rizzo [30] implies that the kernel  $k_E$  is characteristic. Therefore, under the bounded moment conditions by Székely and Rizzo [30], assumption (i) in Theorem 1 is automatically satisfied, implying Theorem 1 holds.

### 3.3 Preliminaries: Problem-driven Scenario Generation

This section discusses problem-driven scenario generation. We highlight two important features that guide our proposed contextual approach. Firstly, we consider computational issues regarding problem-driven scenario generation, followed by concerns caused by non-unique solutions to (2SP-SAA) defined on the surrogate scenarios.

#### Bi-level Problem-driven Scenario Generation

One can attempt to naively employ a bi-level approach to scenario generation based on selecting the scenarios so that the solution of (2SP-SAA), based on said scenarios, minimizes the (2SP) objective. For a given context  $\mathbf{x}$ , this results in the following bi-level problem

$$\min_{\zeta_{1,\dots,K}} L_{\text{task}}(\zeta_{1\dots K}) := h(\mathbf{y}(\zeta_{1\dots K})) + \mathbb{E}_{\omega \sim \mathbb{P}_{\omega|\mathbf{x}}} [q(\mathbf{z}(\mathbf{y}(\zeta_{1\dots K}), \omega), \omega)] \quad (\text{BI-SAA})$$

$$s.t. \quad \mathbf{z}(\mathbf{y}(\zeta_{1\dots K}), \omega) \in \underset{z \in \mathcal{Z}(\mathbf{y}(\zeta_{1\dots K}), \omega)}{\text{argmin}} \quad q(\mathbf{z}, \omega) \quad \forall \omega \in \Omega \quad (\text{SP})$$

$$\mathbf{y}(\zeta_{1\dots K}) \in \underset{\mathbf{y}}{\text{proj}} \underset{\mathbf{y}, z_1, \dots, z_K}{\text{argmin}} \quad h(\mathbf{y}) + \frac{1}{K} \sum_{i=1}^K q(\mathbf{z}_i, \zeta_i) \quad (\zeta\text{-SAA})$$

$$\mathbf{y} \in \mathcal{Y}, \quad \mathbf{z}_i \in \mathcal{Z}(\mathbf{y}, \zeta_i) \quad \forall i \in \{1, \dots, K\},$$

where  $\text{proj}_{\mathbf{y}}$  selects the  $\mathbf{y}$  component of the ( $\zeta$ -SAA) optimal solution set. Some notable aspects of (BI-SAA) exist. First, there is no need for feasibility constraints in the upper-level problem since  $\mathbf{y}(\zeta_{1\dots K})$  is feasible by construction. The lower level problem ( $\zeta$ -SAA) with solution  $\mathbf{y}(\zeta_{1\dots K})$  is the surrogate SAA problem defined on  $K$  scenarios. (BI-SAA) implicitly assumes ( $\zeta$ -SAA) admits a unique solution for any  $\zeta_{1\dots K} \in \Omega^K$ . Similar to (DSG), one can sample a sufficiently large number of scenarios from  $p_\theta(\omega|\mathbf{x})$  and attempt to solve (BI-SAA) with  $\mathbb{P}_{\omega|\mathbf{x}}$  replaced with the empirical measure supported on the samples.

#### Challenges with Gradients

Consider the case where  $\mathbb{P}_{\omega|\mathbf{x}}$  is replaced with  $M$  scenarios. A heuristic approach to solve (BI-SAA) is to use gradients of the upper-level objective with respect to the

upper-level decision variables  $\zeta_{1\dots K}$ . The scenarios can be initialized and updated via gradient descent,  $\zeta \leftarrow \zeta - \eta \partial L_{\text{task}}/\partial \zeta$ , where the chain rule yields

$$\frac{\partial L_{\text{task}}}{\partial \zeta} = \frac{\partial L_{\text{task}}}{\partial \mathbf{y}} \frac{\partial \mathbf{y}}{\partial \zeta} + \frac{\partial L_{\text{task}}}{\partial \mathbf{z}} \frac{\partial \mathbf{z}}{\partial \mathbf{y}} \frac{\partial \mathbf{y}}{\partial \zeta},$$

where  $\mathbf{z} \in \mathbb{R}^{Ms_2}$  refers to the  $M$  second-stage solutions stacked in a vector. The gradient of the upper-level cost relies on computing the gradients of the surrogate problem solution map with respect to the surrogate scenarios  $\frac{\partial \mathbf{y}}{\partial \zeta}$  and the gradients of the subproblem solution map with respect to the first stage solution  $\frac{\partial \mathbf{z}}{\partial \mathbf{y}}$ . These gradients can be computed via various methods depending on the problem structure. For example, in the case of convexity, Agrawal et al. [13]’s `cvxpy` layers can compute the desired gradients. Unfortunately, the gradients are generally sparse and uninformative (even in non-combinatorial problems) [11, 14]. This forms the basis of the proposed problem-driven approach. We mitigate sparse gradients by using neural architectures to smooth out the loss of a particular set of surrogate scenarios and subsequently back-propagate smoothed problem-driven gradients to the task-mapping  $\mathbf{f}$ .

### Non-uniqueness of Optimal Solutions

As written, (BI-SAA) is not well-defined if ( $\zeta$ -SAA) has multiple optimal solutions. A couple of different approaches can address the issue of multiple optimal solutions. In the case that ( $\zeta$ -SAA) is a convex program with a compact feasible set, one can add a small quadratic regularization term  $\epsilon \left( \|\mathbf{y}\|_2^2 + \sum_{i=1}^K \|\mathbf{z}_i\|_2^2 \right)$  to the ( $\zeta$ -SAA) objective to induce strict convexity and hence uniqueness. The unique solution obtained by solving the regularized problem is guaranteed to have objective value within  $\epsilon D^2$  of the optimal objective, where  $D$  is the diameter of the compact feasible set [31]. If ( $\zeta$ -SAA) has a more complex problem structure (e.g., mixed integer constraints), then the regularization trick described above may not be sufficient for uniqueness. We resort to the standard conventions in the bi-level optimization literature [32]. It is unclear which solution to ( $\zeta$ -SAA) is implemented in the upper-level objective. In the classic optimistic (pessimistic) setting, nature selects the optimal solution to ( $\zeta$ -SAA) that minimizes (maximizes) the upper-level objective.

We let  $\mathcal{Y}^*(\zeta_{1\dots K})$  denote the set of  $\mathbf{y}$  that form a part of an optimal solution to ( $\zeta$ -SAA), given  $\zeta_{1\dots K}$  i.e.  $\mathcal{Y}^*(\zeta_{1\dots K}) :=$

$$\left\{ \mathbf{y} \in \mathcal{Y} : h(\mathbf{y}) + \frac{1}{K} \sum_{i=1}^K q(\mathbf{z}_i, \zeta_i) \leq v^*(\zeta_{1\dots K}), \mathbf{z}_i \in \mathcal{Z}(\mathbf{y}, \zeta_i), i \in \{1, \dots, K\} \right\},$$

where  $v^*(\zeta_{1\dots K})$  is the optimal objective value of ( $\zeta$ -SAA). The optimistic version of (BI-SAA) can be written as

$$\min_{\zeta_1, \dots, \zeta_K} \min_{\mathbf{y} \in \mathcal{Y}^*(\zeta_{1\dots K})} h(\mathbf{y}) + \mathbb{E}_{\omega \sim \mathbb{P}_{\omega|\mathbf{x}}} [Q(\mathbf{y}(\zeta_{1\dots K}), \omega)]. \quad (\text{Opt-BI})$$

The optimistic setting assumes that any of the best possible solutions among the optimal solution set  $\mathcal{Y}^*(\zeta_{1\dots K})$  according to  $L_{\text{task}}(\zeta_{1\dots K})$  are selected. One could also consider the pessimistic version; given by replacing  $\min_{\mathbf{y} \in \mathcal{Y}^*(\zeta_{1\dots K})}$  with  $\max_{\mathbf{y} \in \mathcal{Y}^*(\zeta_{1\dots K})}$  in (Opt-BI).

### 3.4 Problem-driven Contextual Scenario Generation

We aim to select  $\mathbf{f} \in \mathcal{F}$  such that, given  $\mathbf{x}$ , the predicted surrogate scenarios  $\mathbf{f}(\mathbf{x})$  produce the highest quality set of optimal ( $\zeta$ -SAA) solutions  $\mathcal{Y}^*(\mathbf{f}(\mathbf{x}))$ . We measure the quality of the optimal solution set  $\mathcal{Y}^*(\mathbf{f}(\mathbf{x}))$  by the best possible two-stage performance among solutions in  $\mathcal{Y}^*(\mathbf{f}(\mathbf{x}))$ . The goal of the problem-driven approach is to select  $\mathbf{f}$  such that  $\mathbf{f}$  is in (Opt-BI)'s solution set (*a.s.*) with respect to  $\mathbb{P}_{\mathbf{x}}$ . This corresponds to

$$\mathbf{f}(\mathbf{x}) \in \underset{\zeta_1, \dots, \zeta_K}{\operatorname{argmin}} \min_{\mathbf{y} \in \mathcal{Y}^*(\zeta_{1\dots K})} h(\mathbf{y}) + \mathbb{E}_{\omega \sim \mathbb{P}_{\omega|\mathbf{x}}} [Q(\mathbf{y}, \omega)]$$

holding (*a.s.*) with respect to  $\mathbb{P}_{\mathbf{x}}$ . Theorem 14.60 due to Rockafellar and Wets [33], implies this is equivalent to  $\mathbf{f}$  being an optimal solution to the following problem

$$\min_{\mathbf{f} \in \mathcal{F}} \mathbb{E}_{\mathbf{x} \sim \mathbb{P}_{\mathbf{x}}} \left[ \min_{\mathbf{y} \in \mathcal{Y}^*(\mathbf{f}(\mathbf{x}))} h(\mathbf{y}) + \mathbb{E}_{\omega \sim \mathbb{P}_{\omega|\mathbf{x}}} [Q(\mathbf{y}, \omega)] \right]. \quad (\text{Opt-PCSG})$$

The following inequality holds

$$\begin{aligned} \min_{\mathbf{y} \in \mathcal{Y}^*(\mathbf{f}(\mathbf{x}))} h(\mathbf{y}) + \mathbb{E}_{\omega \sim \mathbb{P}_{\omega|\mathbf{x}}} [Q(\mathbf{y}, \omega)] &= \min_{\mathbf{y} \in \mathcal{Y}^*(\mathbf{f}(\mathbf{x}))} \mathbb{E}_{\omega \sim \mathbb{P}_{\omega|\mathbf{x}}} [h(\mathbf{y}) + Q(\mathbf{y}, \omega)] \\ &\geq \mathbb{E}_{\omega \sim \mathbb{P}_{\omega|\mathbf{x}}} \left[ \min_{\mathbf{y} \in \mathcal{Y}^*(\mathbf{f}(\mathbf{x}))} h(\mathbf{y}) + Q(\mathbf{y}, \omega) \right], \end{aligned}$$

where the inequality follows by relaxing nonanticipativity among the optimal solution set  $\mathcal{Y}^*(\mathbf{f}(\mathbf{x}))$ . Thus, the following optimistic relaxation of (Opt-PCSG) follows

$$\min_{\mathbf{f} \in \mathcal{F}} \mathbb{E}_{(\mathbf{x}, \omega) \sim \mathbb{P}_{\mathbf{x}, \omega}} \left[ \min_{\mathbf{y} \in \mathcal{Y}^*(\mathbf{f}(\mathbf{x}))} h(\mathbf{y}) + Q(\mathbf{y}, \omega) \right]. \quad (\text{Opt-PCSG}')$$

The advantage of (Opt-PCSG') over (Opt-PCSG) is that it does not require sampling access to  $\mathbb{P}_{\omega|\mathbf{x}}$ . Consequently, (Opt-PCSG') suggests the following loss function

$$\ell_{\text{opt}}(\zeta_{1\dots K}, \omega) := \min_{\mathbf{y} \in \mathcal{Y}^*(\zeta_{1\dots K})} h(\mathbf{y}) + Q(\mathbf{y}, \omega).$$

Evaluating  $\ell_{\text{opt}}(\zeta_{1\dots K}, \omega)$  requires solving ( $\zeta$ -SAA), obtaining the optimal value  $v^*(\zeta_{1\dots K})$ , then given  $\omega$ , finding the solution among  $\mathcal{Y}^*(\mathbf{f}(\mathbf{x}))$  that minimizes  $h(\mathbf{y}) + Q(\mathbf{y}, \omega)$ . The ability to efficiently evaluate  $\ell_{\text{opt}}$  relies on i) the ability to efficiently solve ( $\zeta$ -SAA) on  $K$  scenarios (Assumption 2), and ii) the ability to efficiently minimize the 2SP objective defined by a single scenario  $\omega$  over the optimal solution set  $\mathcal{Y}^*(\mathbf{f}(\mathbf{x}))$ .

Suppose ( $\zeta$ -SAA) obtains optimal value  $v^*(\zeta_{1\dots K})$ , then evaluating  $\ell_{\text{opt}}(\zeta_{1\dots K}, \omega)$  is equivalent to

$$\begin{aligned} \ell_{\text{opt}}(\zeta_{1\dots K}, \omega) &= \min_{\mathbf{y}, \mathbf{z}, \mathbf{z}_1, \dots, \mathbf{z}_K} h(\mathbf{y}) + q(\mathbf{z}, \omega) && \text{(Opt-Search)} \\ \text{s.t. } & h(\mathbf{y}) + \frac{1}{K} \sum_{i=1}^K q(\mathbf{z}_i, \zeta_i) \leq v^*(\zeta_{1\dots K}) && (1) \\ & \mathbf{y} \in \mathcal{Y}, \mathbf{z} \in \mathcal{Z}(\mathbf{y}, \omega), \mathbf{z}_i \in \mathcal{Z}(\mathbf{y}, \zeta_i), \forall i \in \{1, \dots, K\}. \end{aligned}$$

(**Opt-Search**) has the same constraints as ( $\zeta$ -SAA), along with constraint (1) that ensures the optimality of  $(\mathbf{y}, \mathbf{z}_1, \dots, \mathbf{z}_K)$  with respect to ( $\zeta$ -SAA). An additional decision variable  $\mathbf{z}$  is introduced to model the recourse in response to scenario  $\omega$ . In addition to linear programs and convex programs with multiple solutions, the optimistic approach is generally amenable to mixed-integer programs (MIP) with convex relaxations since, in this case, the resulting instance of (**Opt-Search**) is a convex MIP with one additional constraint (1) and decision variable  $\mathbf{z}$ .

In the case where ( $\zeta$ -SAA) exhibits unique solutions,  $\ell_{\text{opt}}$  reduces to the simplified loss function  $h(\mathbf{y}(\zeta_{1\dots K})) + Q(\mathbf{y}(\zeta_{1\dots K}), \omega)$  whose evaluation only requires solving ( $\zeta$ -SAA) (Assumption 2) and a single subproblem (SP) (Assumption 1) to obtain  $\mathbf{y}(\zeta_{1\dots K})$  and  $\mathbf{z}(\mathbf{y}(\zeta_{1\dots K}), \omega)$ , respectively. Furthermore, if solving (**Opt-Search**) proves too computationally burdensome, then one can easily compute  $h(\mathbf{y}(\zeta_{1\dots K})) + Q(\mathbf{y}(\zeta_{1\dots K}), \omega)$  as a heuristic loss (although learning may not be well-defined in this case). This work uses  $\ell_{\text{opt}}$  for all problems under consideration since they lack uniqueness guarantees and are amenable to direct computation by solving (**Opt-Search**). Like the optimistic case, one can consider the pessimistic case. Following the same line of reasoning suggests  $\max_{\mathbf{y} \in \mathcal{Y}^*(\zeta_{1\dots K})} h(\mathbf{y}) + Q(\mathbf{y}, \omega)$  as a loss function. However, evaluating this loss is more difficult than evaluating  $\ell_{\text{opt}}$ . For instance, in the case of a two-stage linear program, evaluating the pessimistic loss is equivalent to maximizing a convex function. Due to this added complexity, this work considers the optimistic case.

### 3.5 Solution Methodology

Thus far, two loss functions have been introduced. In the case of  $\ell_{\text{MMD}}$ , empirical risk minimization over a parametric class  $\mathbf{f}_\phi$ ,  $\phi \in \Phi$  via gradient-based methods is straightforward. We will typically take  $\Phi$  as a class of neural networks. More details are provided in the experimental section. As discussed in Section 3.3,  $\ell_{\text{opt}}$  will in general exhibit sparse gradients with respect to the output of  $\mathbf{f}_\phi$ , making back-propagation of gradients ineffective. To address this, a neural network architecture (Loss-Net) is proposed to approximate the problem-based loss  $\ell_{\text{opt}}$ .

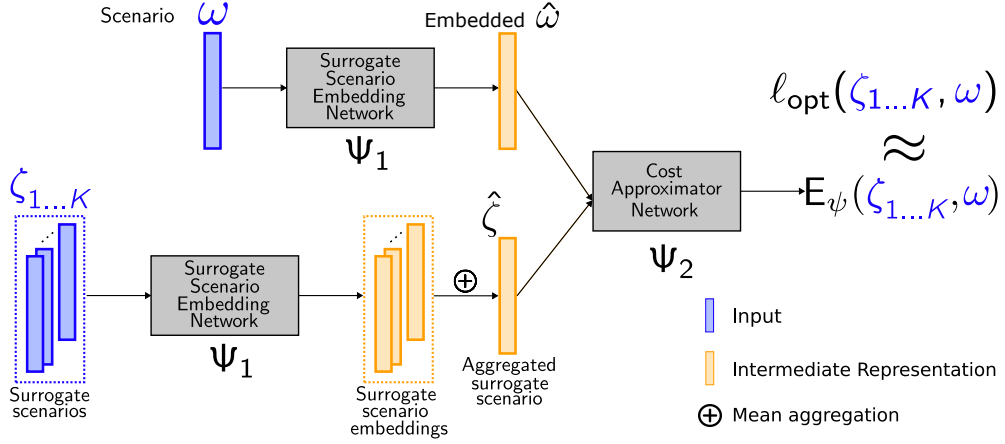
The network is a mapping  $E_\psi$  from  $\Omega^{K+1} \rightarrow \mathbb{R}$  with the aim that  $E_\psi(\zeta_{1\dots K}, \omega) \approx \ell_{\text{opt}}(\zeta_{1\dots K}, \omega)$ . The architecture is shown in Figure 3. The architecture's design is motivated by permutation invariant neural architectures [34, 35]. In particular, Patel et al. [3]'s Neur2SP architecture is notable since they also apply permutation invariant neural architectures to 2SPs. The network embeds each surrogate scenario  $\zeta_k$ ,  $k \in [K]$

into a latent space  $\Omega' \subseteq \mathbb{R}^{\text{latent}}$  using an encoder  $\Psi_1 : \Omega \rightarrow \Omega'$ . The embedded surrogate set is then represented as a single encoded scenario  $\hat{\zeta}$  via mean aggregation i.e.,  $\hat{\zeta} = \frac{1}{K} \sum_{k=1}^K \Psi_1(\zeta_k)$ . This ensures that the predictions from the network are invariant to the ordering of the input set  $\zeta_{1\dots K}$ . The input scenario is also embedded via  $\Psi_1$ :  $\hat{\omega} = \Psi_1(\omega)$ . The embedding of the surrogate scenarios  $\hat{\zeta}$  and embedded input scenario  $\hat{\omega}$  are fed into a separate network  $\Psi_2 : \Omega' \times \Omega' \rightarrow \mathbb{R}$  that outputs the approximation of  $\ell_{\text{opt}}(\zeta_{1\dots K}, \omega)$  given by

$$E_\psi(\zeta_{1\dots K}, \omega) = \Psi_2 \left( \hat{\zeta}, \hat{\omega} \right) = \Psi_2 \left( \frac{1}{K} \sum_{k=1}^K \Psi_1(\zeta_k), \Psi_1(\omega) \right).$$

The networks,  $\Psi_1$  and  $\Psi_2$ , are taken to be fully connected feedforward neural networks with Rectified Linear Unit (ReLU) activations of appropriate input and output dimensions, each with hyperparameters such as the numbers of hidden layers and activations.

**Fig. 3** Loss-Net Architecture



It would be ideal for  $\ell_{\text{opt}}$  to be representable via a structure similar to  $E_\psi$ . Indeed, the following proposition shows that  $\ell_{\text{opt}}$  can be represented as a composition of functions like  $E_\psi$  when the scenario embedding space  $\Omega'$  is of large dimensionality.

**Proposition 2.** For a fixed positive integer  $K$ , the (continuous) task-based loss  $\ell_{\text{opt}} : \Omega^K \times \Omega \rightarrow \mathbb{R}$ , where  $\Omega \subseteq \mathbb{R}^p$  is compact, satisfies

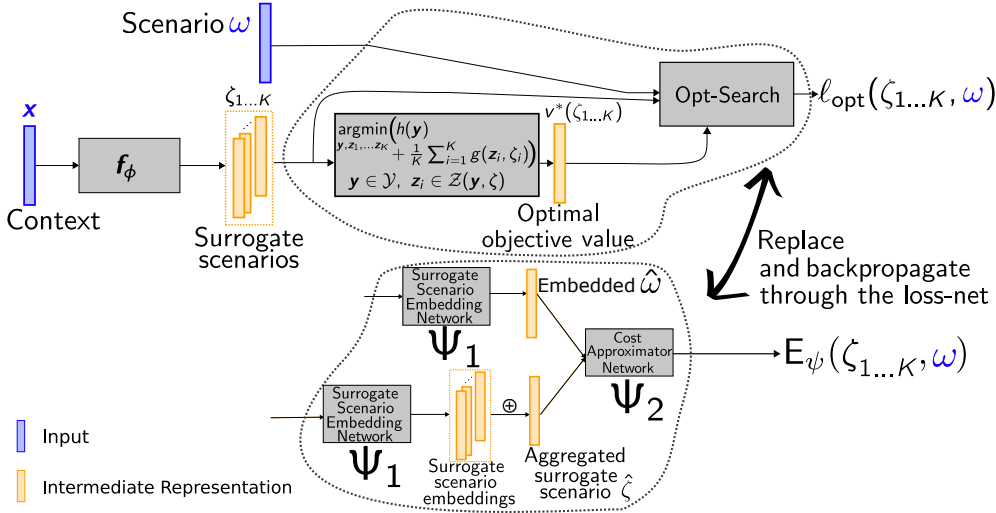
$$\ell_{\text{opt}}(\zeta_{1\dots K}, \omega) = \rho \left( \frac{1}{K} \sum_{k=1}^K \tau(\zeta_k), \tau(\omega) \right) \quad \forall \zeta_{1\dots K} \in \Omega^K, \omega \in \Omega,$$

with continuous  $\tau : \mathbb{R}^p \rightarrow \mathbb{R}^{\binom{K+p}{p}-1}$ , (continuous)  $\rho : \mathbb{R}^{\binom{K+p}{p}-1} \times \mathbb{R}^{\binom{K+p}{p}-1} \rightarrow \text{codom}(\rho)$ , and  $\text{codom}(\ell_{\text{opt}}) \subseteq \text{codom}(\rho)$

The proof of Proposition 2 is a direct application of Proposition 1 by Tabaghi and Wang [35]. The proof introduces additional notation and is provided in Appendix B. Given the representation provided by Proposition 2, approximating  $\ell_{\text{opt}}$  by  $E_\psi$  amounts to replacing  $\rho$  and  $\tau$  with fully connected feedforward ReLU networks  $\Psi_2$  and  $\Psi_1$ , respectively. Proposition 2 produces a representation such that the continuity of  $\ell_{\text{opt}}$  determines the continuity of  $\rho$ . At the same time,  $\tau$  is continuous, independent of the continuity of  $\ell_{\text{opt}}$ . In any case, by using neural architectures, we leverage a continuous approximation to  $\ell_{\text{opt}}$ , irrespective of whether  $\ell_{\text{opt}}$  is continuous by simply replacing  $\rho$  with  $\Psi_2$ . Furthermore, the representation in Proposition 2 has  $\Omega' \subseteq \mathbb{R}^{\binom{K+p}{p}-1}$ , i.e. leverages a high-dimensional embedding of the scenarios.

The loss network acts as replacement for  $\ell_{\text{opt}}(\zeta_{1\dots K}, \omega)$ . The basic idea underpinning the proposed approach is to replace  $\ell_{\text{opt}}(\zeta_{1\dots K}, \omega)$  with  $E_\psi(\zeta_{1\dots K}, \omega)$  and use it to learn  $\mathbf{f}_\phi$ . This idea is visually depicted in Figure 4. Given a trained  $E_\psi$ , one can use it to infer  $\zeta_{1\dots K}$  via gradient-based minimization. The remainder of this section describes training procedures to learn  $E_\psi$  and  $\mathbf{f}_\phi$ .

**Fig. 4** Replacing  $\ell_{\text{opt}}$  with  $E_\psi$



*Note.* Replace the true downstream loss with the task-net approximated loss to avoid sparse gradients

## Static Approach

We do not seek to construct  $E_\psi$  such that it uniformly approximates  $\ell_{\text{opt}}$  over  $\Omega^{K+1}$ . Instead, we wish to approximate  $\ell_{\text{opt}}$  over a distribution  $\mathbb{P}_{\zeta_1, \dots, \zeta_K, \omega}$  that is reflective of the surrogate scenarios  $\zeta_{1\dots K}$  and uncertainty that  $E_\psi$  will encounter in practice. Once trained,  $E_\psi$  is used to guide the learning for  $\mathbf{f}_\phi$ . We refer to this approach as the static approach.

A simple approach is to train  $E_\psi$  over surrogate scenarios produced by  $\zeta_{1\dots K} = \hat{\mathbf{f}}_{\text{MMD}}(\mathbf{x})$ , where  $\hat{\mathbf{f}}_{\text{MMD}}$  denotes the task-mapping obtained via minimization of  $\mathcal{L}_{\text{MMD}}$  over the iid sample  $S$ . Given  $\hat{\mathbf{f}}_{\text{MMD}}$ , the sample for training  $E_\psi$  is generated by forming the surrogate scenarios  $\zeta_{1\dots K}^{(i)} = \hat{\mathbf{f}}_{\text{MMD}}(\mathbf{x}^{(i)})$ , and finally evaluating the task-based loss  $\ell_{\text{opt}}^{(i)} = \ell_{\text{opt}}(\zeta_{1\dots K}^{(i)}, \omega^{(i)})$ , yielding a dataset  $S' = \{(\mathbf{x}^{(i)}, \zeta_{1\dots K}^{(i)}, \omega^{(i)}, \ell_{\text{opt}}^{(i)})\}_{i=1}^n$ .  $E_\psi$  is trained by gradient-based methods to minimize the prediction error over  $S'$

$$\min_{\psi} \frac{1}{n} \sum_{i=1}^n \left( E_\psi(\zeta_{1\dots K}^{(i)}, \omega^{(i)}) - \ell_{\text{opt}}^{(i)} \right)^2,$$

where it is assumed that hyperparameters associated with the learning procedure, such as optimizer learning rates, batch size, and  $l_2$  regularization on the weights, can be set such that the resulting loss-net achieves generalization. The resulting loss approximator, obtained from training over  $S'$  is denoted by  $\hat{E}$ .

Although it is tempting to select the task-net to minimize the approximate task loss over a sample, we observed that optimizing the approximate task loss tended to yield surrogate scenario predictions  $\mathbf{f}_\phi(\mathbf{x})$  that are far from the distribution of the samples used to train the loss network. I.e., directly minimizing the approximate task loss tends to yield a task-net whose predictions maximize the error of the approximate task loss (*loss error maximization*). To mitigate this, we proposed regularizing the approximate task loss by the MMD loss to select  $\mathbf{f}_\phi$

$$\min_{\phi} \frac{1}{n} \sum_{i=1}^n \hat{E}(\mathbf{f}_\phi(\mathbf{x}^{(i)}), \omega^{(i)}) + \lambda \ell_{\text{MMD}}(\mathbf{f}_\phi(\mathbf{x}^{(i)}), \omega^{(i)}), \quad (\text{Static-PCSG})$$

where  $\lambda \geq 0$  is a regularization penalty. The MMD regularization ensures that the surrogate scenario predictions do not stray too far from the input distribution used to train the loss net. Furthermore, the proposed problem is amenable to empirical risk minimization via the sample  $S$ , making training straightforward. Once  $\hat{E}_\psi$  is trained, one can input any number of surrogate scenarios into  $\Psi_1$ , and a numerical result will still be produced. Although we do not explore it here, this can potentially reduce training time by using an  $\hat{E}_\psi$  that is trained via cheaper evaluations of  $\ell_{\text{opt}}$  using  $K' < K$  surrogate scenarios. The static approach for selecting  $\mathbf{f}_\phi$  is shown in Algorithm 1. We denote the task network obtained by training on  $S'$  by  $\hat{\mathbf{f}}_{\text{PCSG}}$ .

### Dynamic Approach

After running Algorithm 1, there is a trained task-net  $\hat{\mathbf{f}}_{\text{PCSG}}$  and loss-net  $\hat{E}$ . By construction,  $\hat{E}$  approximates  $\ell_{\text{opt}}$  over the distribution of inputs  $(\hat{\mathbf{f}}_{\text{MMD}}(\mathbf{x}), \omega)$ , where  $(\mathbf{x}, \omega) \sim \mathbb{P}_{\mathbf{x}, \omega}$ . However, there is no guarantee that  $\hat{E}$  approximates  $\ell_{\text{opt}}$  over the analogous distribution induced by  $\hat{\mathbf{f}}_{\text{PCSG}}$ . Thus, additional samples for the loss-net are generated using  $\hat{\mathbf{f}}_{\text{PCSG}}$ , by forming the surrogate scenarios  $\zeta_{1\dots K}^{(i)} = \hat{\mathbf{f}}_{\text{PCSG}}(\mathbf{x}^{(i)})$ , and evaluating the task-based loss  $\ell_{\text{opt}}^{(i)} = \ell_{\text{opt}}(\zeta_{1\dots K}^{(i)}, \omega^{(i)})$ . The resulting samples, in



---

**Algorithm 1** Training and Using  $E_\psi$  for Static PCSG

---

**Require:** Loss function  $\ell_{\text{opt}}$ , regularization parameter  $\lambda$ , Network architecture and training parameters (e.g. batch size ( $B$ ), number of epochs ( $E$ ), No. hidden units), Sample  $S = \{(\mathbf{x}^{(i)}, \omega^{(i)})\}_{i=1}^n$ , Trained MMD network  $\hat{\mathbf{f}}_{\text{MMD}}$

- 1: Initialize networks  $E_\psi$  and  $\mathbf{f}_\phi$  and hyperparameters: e.g. batch size ( $B$ )
- 2: **for** each  $(\mathbf{x}^{(i)}, \omega^{(i)}) \in S$  **do**
- 3:   Evaluate  $\zeta_{1\dots K}^{(i)} = \hat{\mathbf{f}}_{\text{MMD}}(\mathbf{x}^{(i)})$ ,  $\ell_{\text{opt}}^{(i)} = \ell_{\text{opt}}(\zeta_{1\dots K}^{(i)}, \omega^{(i)})$
- 4: **end for**
- 5: Form dataset  $S' = \{(\zeta_{1\dots K}^{(i)}, \omega^{(i)}, \ell_{\text{opt}}^{(i)})\}_{i=1}^n$
- 6: Train  $\hat{E}$  over  $S'$ :  $\min_\psi \frac{1}{|S'|} \sum_{\zeta_{1\dots K}, \omega, \ell_{\text{opt}} \in S'} (E_\psi(\zeta_{1\dots K}, \omega) - \ell_{\text{opt}})^2$ , yielding  $\hat{E}$
- 7: Solve (Static-PCSG) over  $S$  using  $\hat{E}$
- 8: **Output:** Trained task-net  $\hat{\mathbf{f}}_{\text{PCSG}}$  and loss-net  $\hat{E}$

---

addition to the sample generated by  $\hat{\mathbf{f}}_{\text{MMD}}$  then can be used to train  $\hat{E}$  further. Once  $\hat{E}$  is updated, resolving (Static-PCSG) updates the task-mapping. The repetition of this process for  $T$  iterations is referred to as the dynamic approach and is summarized in Algorithm 2.

---

**Algorithm 2** Dynamic Training Algorithm for  $E_\psi$  and  $\mathbf{f}_\phi$ 

---

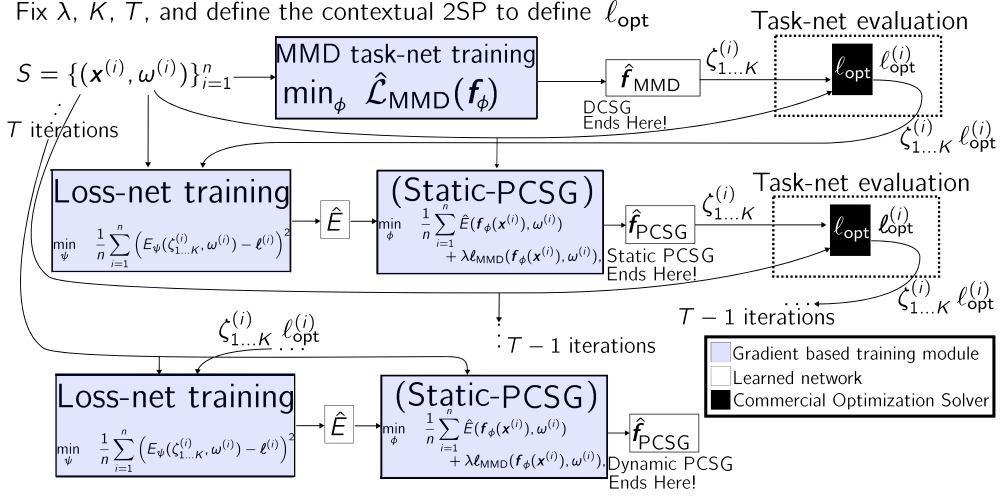
**Require:** Same inputs as Algorithm 1, iteration limit  $T$

- 1: Perform steps 1-5 in Algorithm 1, yielding  $S'$ ,  $\hat{E}$  and  $\hat{\mathbf{f}}_{\text{PCSG}}$
- 2: **for**  $t = 1 \dots T$  **do**
- 3:   **for** each  $(\mathbf{x}^{(i)}, \omega^{(i)}) \in S$  **do**
- 4:     Evaluate  $\zeta_{1\dots K}^{(i)} = \hat{\mathbf{f}}_{\text{PCSG}}(\mathbf{x}^{(i)})$ ,  $\ell_{\text{opt}}^{(i)} = \ell_{\text{opt}}(\zeta_{1\dots K}^{(i)}, \omega^{(i)})$
- 5:      $S' \leftarrow S' + \{(\zeta_{1\dots K}^{(i)}, \omega^{(i)}, \ell_{\text{opt}}^{(i)})\}_{i=1}^n$    ▷ Replay buffer: keep past  $T' < T$  iterations
- 6:   **end for**
- 7:   Update  $\hat{E}$  over  $S'$ :  $\min_\psi \frac{1}{|S'|} \sum_{\zeta_{1\dots K}, \omega, \ell_{\text{opt}} \in S'} (E_\psi(\zeta_{1\dots K}, \omega) - \ell_{\text{opt}})^2$
- 8:   Fix  $\hat{E}$  and update  $\mathbf{f}_\phi$  via (Static-PCSG) over  $S$  using  $\hat{E}$
- 9: **end for**
- 10: **Output:** Trained task-net  $\hat{\mathbf{f}}_{\text{PCSG}}$  and loss-net  $\hat{E}$

---

Algorithm 2 is similar to the approach proposed by Zharmagambetov et al. [11]. In the case of scenario generation, we observe that Zharmagambetov et al. [11]’s approach fails without the use of MMD regularization. Thus, the implicit use of MMD to initialize the samples for  $E_\psi$  and regularize the task-mapping  $\mathbf{f}_\phi$  constitutes a critical difference between this work and theirs. Similar to Zharmagambetov et al. [11], the proposed methods do not maintain the entire history of examples for training  $E_\psi$  at every iteration and instead, a *replay buffer* [36] is used, keeping, at most, the last  $T = 3$  iterations of data. Furthermore, Algorithm 2, builds upon Algorithm 1, which relies upon empirical minimization of  $\mathcal{L}_{\text{MMD}}(\mathbf{f}_\phi)$ . Figure 5 visually displays the entire training process and the relationships between DCSG, Static PCSG, and Dynamic PCSG.

**Fig. 5** Visual representation of the DCSG and PCSG training procedures



The experimental results will evaluate the performance of these three approaches relative to each other. In terms of training, minimizing  $\hat{\mathcal{L}}_{\text{MMD}}(\mathbf{f}_{\phi})$  has the advantage that no optimization problems are required to evaluate the loss. However, the MMD approach does not consider the problem structure of (2SP-SAA). The static and dynamic approaches have the advantage of considering the downstream decision loss associated with a particular choice of  $\mathbf{f}$ . The static approach has the benefit over the dynamic approach that the training of  $E_{\psi}$ , and thus the repeated solution of optimization problems to evaluate  $\ell_{\text{opt}}$  need only be performed once. While the dynamic approach offers an advantage over the static approach by aiming to construct better approximations of  $\ell_{\text{opt}}$  near the chosen  $\mathbf{f}$ , it also has a drawback. Specifically, computations of  $\ell_{\text{opt}}$  must be performed at each iteration to update the loss-net.

## 4 Experiments

This section applies the proposed CSG approaches to four contextual 2SP settings. We relegate details regarding the computing setup and software used to Appendix C.1.

### 4.1 Newsvendor

**Problem Setting:** The classic newsvendor problem is used to illustrate the proposed approach. Each day, a newsvendor purchases  $y$  newspapers at unit-cost  $c$ . The vendor is budget-constrained, so they can only purchase at most  $u$  papers. After purchasing, the vendor sells as many papers as possible for a unit price of  $q$ . When the day is done, the vendor can return the papers at a salvage price  $r < c$ . Suppose the vendor observes contextual information  $\mathbf{x}$  before purchasing the paper. For example,  $\mathbf{x}$  could represent the day of the week, the weather, and sales from previous days. The demand for the

papers  $\omega$  is unknown at the time of purchase. Thus, the newsvendor wishes to solve

$$\min_y cy + \mathbb{E}_{\omega \sim \mathbb{P}_{\omega|\mathbf{x}}} [Q(y, \omega)] \quad s.t. \quad y \in [0, u], \quad (2)$$

where  $Q(y, \omega) = \min_{z \geq 0, w \geq 0} -qz - rw \quad s.t. \quad z \leq \omega, z + w \leq y$ . The decision variables  $z$  and  $w$  represent the quantities of papers sold and salvaged, respectively. We consider the following problem parameter setting  $(c, q, r, u) = (1.0, 1.05, 0.1, 60.0)$ .

**Experimental Setup:** A synthetic environment is used for evaluation purposes.  $\mathbf{x}$  is set to be distributed according to a two-dimensional normal distribution. A randomly initialized neural network  $\mathbf{f}_{\text{Random}} : \mathcal{X} \rightarrow \mathbb{R}_+^{200}$  is used to map  $\mathbf{x}$  to an empirical demand distribution  $\mathbb{P}_{\omega|\mathbf{x}}$  supported on 200 points. The resulting joint distribution has an expectation of 15.1 and a standard deviation of 0.25 units.

The decision maker has a dataset of  $n = 500$  samples of  $\mathbf{x}$  and  $\omega$ . The **DCSG**, **Static-PCSG**, and **Dynamic-PCSG** approaches are trained on this sample. In figures and tables, we label these approaches as *MMD*, *Static* and *Dynamic*. All approaches let  $\mathbf{f}_\phi$  be parameterized as a fully connected feedforward neural network with ReLU activation, mapping  $\mathbf{x}$  to  $\mathbb{R}_+^K$ . We select the architecture by considering the **DCSG** problem. A random search over a single training sample determines hyperparameters such as the number of hidden layers, number of units, and optimizer parameters. It optimizes  $\hat{\mathcal{L}}_{\text{MMD}}$  on a fixed hold out of 20% of the training samples. The loss network  $E_\psi$ 's architecture is selected similarly. First,  $\hat{\mathbf{f}}_{\text{MMD}}$ , is used to generate the dataset  $\{\zeta_{1 \dots K}^{(i)}, \omega^{(i)}, \ell_{\text{opt}}^{(i)}\}_{i=1}^n$ , then a similar hold out procedure is used to select the architecture. The loss network  $E_\psi$  is selected to be the same in both the static and dynamic approaches. We take this approach to selecting the network architectures in all the experiments considered in this work.

After training, **DCSG**, **Static-PCSG** and **Dynamic-PCSG** are evaluated by considering  $n_{\text{val}} = 100$  out-of-sample contextual observations  $\{\mathbf{x}_{\text{val}}^{(i)}\}_{i=1}^{n_{\text{val}}}$ , and associated distributions  $\{\mathbb{P}_{\omega|\mathbf{x}_{\text{val}}^{(i)}}\}_{i=1}^{n_{\text{val}}}$ . Given a task-mapping  $\mathbf{f}$  along with an observation  $\mathbf{x}^{(i)}$ , ( $\zeta$ -SAA) is solved using the predicted surrogate scenarios  $\zeta_{1 \dots K}^{(i)} = \mathbf{f}(\mathbf{x}^{(i)})$ . A resulting first-stage solution is then evaluated using the 2SP objective with the expected recourse calculated using  $\mathbb{P}_{\omega|\mathbf{x}^{(i)}}$ . Additionally, we also calculated the 2SP loss where the (**Opt-Search**) objective is replaced with the 2SP objective defined by  $\mathbb{P}_{\omega|\mathbf{x}^{(i)}}$  and observed no difference between the two ways to evaluate solutions produced by  $\mathbf{f}$ . Let  $v_{\text{MMD}}^{(i)}$ ,  $v_{\text{Static}}^{(i)}$ , and  $v_{\text{Dynamic}}^{(i)}$  denote the objectives for the  $i$ th validation observation for **DCSG**, **Static-PCSG** and **Dynamic-PCSG** respectively. The optimal newsvendor solution is also computed using  $\mathbb{P}_{\omega|\mathbf{x}_{\text{val}}^{(i)}}$  with optimal objective value denoted by  $v_{2\text{SP}}^{(i)}$ .

We consider two additional benchmarks. The first considers the expected value solution, determined by considering the newsvendor problem with a single scenario given by  $\mathbb{E}[\omega|\mathbf{x}]$ . In practice, the conditional mean is not known, so this is a benchmark that cannot be implemented. Considering the expected value solution allows us to ascertain whether the proposed methodologies can unlock the value of the stochastic solution [37]. The second benchmark is a quantile regression approach. It is well known

that the optimal solution to the newsvendor is

$$y^* = \begin{cases} 0 & \text{if } \frac{q-c}{q-r} < F_{\mathbb{P}}(0), \\ u & \text{if } \frac{q-c}{q-r} > F_{\mathbb{P}}(u), \\ F_{\mathbb{P}}^{-1}\left(\frac{q-c}{q-r}\right) & \text{otherwise.} \end{cases},$$

where  $F_{\mathbb{P}}$  is the cumulative density according to  $\mathbb{P}$  and  $F_{\mathbb{P}}^{-1}(\alpha)$  is the  $\alpha$  quantile of  $F$ . This suggests a quantile estimation approach to obtain a linear model  $F_{\mathbb{P}_{\omega|\mathbf{x}}}^{-1}\left(\frac{q-c}{q-r}\right) = \beta^{\top} \mathbf{x}$ , from the training sample. The quantile estimation approach is well-studied in newsvendor problems. Liu et al. [38] point out that quantile estimation is equivalent to determining the optimal linear (in  $\mathbf{x}$ ) purchasing policy that minimizes the opportunity cost over the sample. The quantile regression (QR) is performed using the `stats-models` package [39] that implements QR as in [40]. Let  $v_{\mathbb{E}[\omega|\mathbf{x}]}^{(i)}$  and  $v_{\text{QR}}^{(i)}$  denote the task losses for the solutions obtained via the expected value and QR approaches respectively for the  $i$ th validation sample.

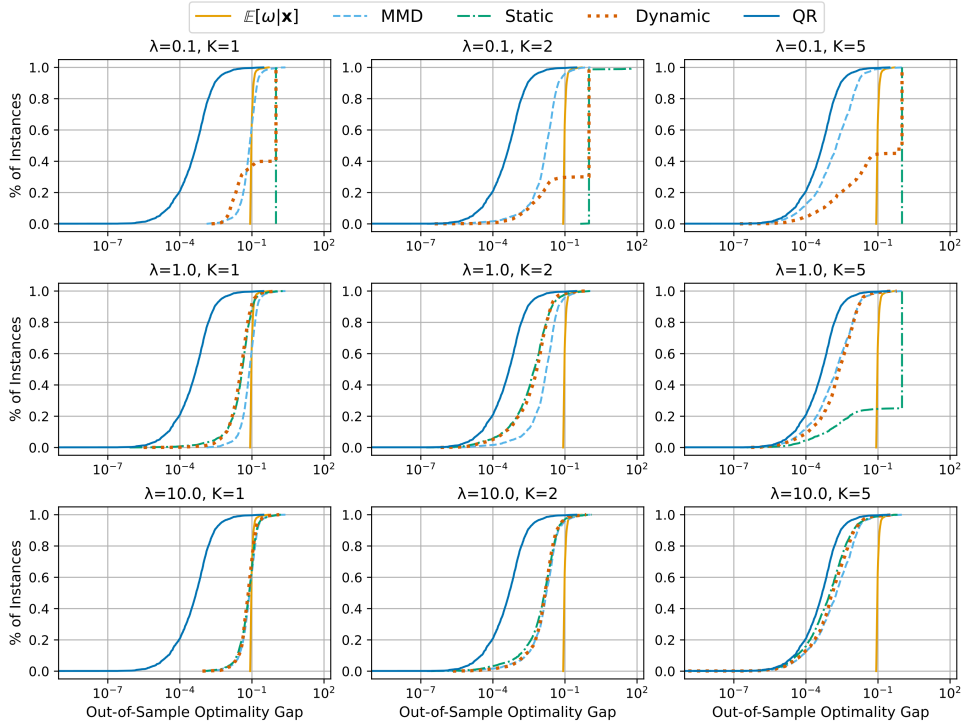
In this experiment  $K$  varies in  $\{1, 2, 5\}$ , along with the MMD regularization parameter  $\lambda \in \{10^{-1}, 10^0, 10^1\}$  to determine how the proposed approaches compare against the benchmarks. The experiment consists of  $n_{\text{trials}} = 20$  trials. In each trial, a training set of  $n$  joint observations and the evaluation set of  $n_{\text{eval}}$  contexts and conditional distributions are sampled. Each approach is trained and evaluated. For each trial and validation instance, the optimality gap for each method is calculated as

$$\text{Gap}_m = (v_m - v_{2\text{SP}})/|v_{2\text{SP}}|, \quad m \in \{\mathbb{E}[\omega|\mathbf{x}], \text{MMD}, \text{Static}, \text{Dynamic}, \text{QR}\}.$$

**Results:** Figure 6 shows the cumulative distribution function (CDF) of the optimality gaps for each method by  $K$  and  $\lambda$  evaluated over the validation instances. If  $(x, y)$  lies on the curve, the method achieves an optimality gap no more than  $10^x$  on  $100y\%$  of problems on the validation sets over all the trials. As expected, the quantile regression approach performs the best as it explicitly uses the samples to predict the closed-form solution to the contextual newsvendor problem. The MMD approach captures more of the value of the stochastic solution as  $K$  is increased. However, the MMD approach has the downside that when  $K = 1$ , it reduces to conditional mean estimation via least-squares and, as such, is unlikely to offer any value over the expected value solution on average (since the expected value solution is the associated Bayes optimal predictor).

The task-based approaches yield poorly performing scenario mappings when  $\lambda = 0.1$ . In this setting, the dynamic approach slightly improves on the static approach. Furthermore, the MMD approach outperforms when the task-based approaches lack regularization. When  $K \in \{1, 2\}$  and  $\lambda = 1.0$ , the task-based approaches out-perform MMD significantly. Of the CSG approaches, the best-performing approaches when  $K \in \{1, 2\}$  are the task-based approaches with  $\lambda = 1.0$ , and when  $K = 5$ , the best-performing approaches are the task-based approaches with  $\lambda = 10$ . However, when  $K = 5$ , the MMD approach is competitive with the task-based approaches. Furthermore, when  $K > 1$ , and  $\lambda \geq 1.0$ , the CSG approaches consistently exhibit value over

**Fig. 6** Out of sample optimality gaps for the contextual newsvendor problem.



the expected value solution. Lastly, task-based CSG outperforms the expected value solution when  $K = 1$ ,  $\lambda = 1.0$ .

Overall, task-based approaches offer more value than the MMD approach for smaller values of  $K$ . However, for larger  $K$ , the MMD approach can obtain higher-quality solutions. The importance of distributional regularization is also readily apparent, allowing PCSG methods to outperform DCSG significantly for small values of  $K \leq 2$ . Learning the surrogate scenario mapping for ( $\zeta$ -SAA) in a purely task-driven manner does not yield mappings that produce high-quality solutions. Although the QR approach exhibits the best performance, CSG methods still display desirable performance. Furthermore, CSG can be applied independently of the problem structure. The remaining experiments consider problem settings that are not endowed with a prescribed problem-driven approach to contextual optimization.

## 4.2 Capacity Planning (CEP1)

**Problem Setting:** Next, we test CSG via a contextual version of the CEP1 problem discussed in the introduction. In this application, the production manager wishes to decide the total hours of added capacity  $\mathbf{y}_{\text{cap}} \in \mathbb{R}_+^{n_{\text{machines}}}$  and hours of operation  $\mathbf{y}_{\text{op}} \in \mathbb{R}_+^{n_{\text{machines}}}$  to meet uncertain demand for the  $m$  parts  $\omega \in \mathbb{R}_+^m$ . The detailed formulation of the CEP1 problem is relegated to Appendix C.2.1.

**Experimental Setup:** Similar to the newsvendor, we consider a randomly initialized neural network to generate the conditional distribution  $\mathbb{P}_{\omega|\mathbf{x}}$  for context  $\mathbf{x}$ . The procedure used to define the underlying  $\mathbb{P}_{\omega|\mathbf{x}}$  is described in Appendix C.2.2. The experimental setup is nearly identical to that of the newsvendor. Table 1 contains the CEP1 experiment parameters.

**Table 1** Summary of CEP1 Experimental Parameters

Parameter	Value
Number of samples ( $n$ )	500
Number of out-of-sample instances ( $n_{eval}$ )	200
Number of surrogate scenarios ( $K$ )	$\{1, 2, 5\}$
MMD regularization ( $\lambda$ , scaled by $\hat{\mathcal{L}}_{\text{MMD}}$ )	$\hat{\mathcal{L}}_{\text{MMD}} * \tilde{\lambda}$ where $\tilde{\lambda} \in \{10^{-3+i}\}_{i=1}^4$
Number of sampling repetitions ( $n_{\text{trials}}$ )	20
Number of loss-net updates in dynamic PCSG ( $T$ )	4

The resulting 2SP is a two-stage linear program; thus, there are no guarantees for uniqueness. Furthermore, the task-net  $\mathbf{f}_\phi$  is parameterized as a fully connected feedforward neural network with ReLU activation, mapping  $\mathbf{x}$  to  $\mathbb{R}_+^{m \times K}$ .

**Results:** The CDF of the optimality gap for each method, by  $K$  and  $\lambda$  is relegated to Appendix C.2.3 for space considerations. Table 2 shows the median optimality gaps over all the validation instances and trials. We observe in this setting that the value of considering stochastic solutions is not large since the expected value solution attains a median optimality gap of 1.69%. Unlike the newsvendor, the MMD approach does not yield solutions that are closer to optimal as  $K$  increases, yielding some evidence of an overfitting effect for large  $K$ . Although the MMD approach still underperforms the expected value solutions when  $K = 1$ . In settings where  $\lambda \geq 0.1$ , the dynamic approach consistently improves on the static approach, highlighting the performance gains obtained by iteratively refining the loss-net via the dynamic approach. When  $(K, \tilde{\lambda}) = (1, 0.01)$ , the PSCR methods attain smaller optimality gaps than the other methods and can unlock the value of stochastic solution with a single scenario. When  $K \geq 2$ , the PCSG methods perform similarly to MMD.

Table 3 compares the performance of the different methods across  $K$  by showing the percentage of instances in which the particular method obtains the lowest out-of-sample 2SP cost (the columns sum to 100%). When  $K = 1$ , the MMD (regression) approach never achieves the lowest 2SP objective. Knowing the true conditional expectation yields the best solution in only 11.6% of instances. In contrast, the static and dynamic methods outperform when  $\lambda = 0.01$ , achieving the lowest cost in 29.8% and 55.7% of instances, respectively. When  $K = 2$  (5), the MMD approach becomes more competitive, obtaining the lowest 2SP cost in 15.1% (11.7%) instances. Still, when  $K \in \{2, 5\}$ , the dynamic approach with  $\tilde{\lambda}$  obtains the best objective most often. Like the contextual newsvendor, task-based approaches offer more value than the MMD approach for smaller values of  $K$ . Although the MMD approach can obtain higher-quality solutions for larger  $K$ , with appropriate regularization, task-driven approaches tend to obtain the best results more often.

**Table 2** (CEP1) Median optimality gaps on validation instances for various methods

	$K = 1$	$K = 2$	$K = 5$
$\mathbb{E}[\omega \mathbf{x}]$	1.69%	1.69%	1.69%
MMD	2.36%	0.43%	0.76%
$\tilde{\lambda}$	<b>Static</b>		
0.01	1.50%	5.04%	6.31%
0.1	2.07%	1.23%	1.20%
1	2.31%	0.44%	0.65%
10	2.36%	0.39%	0.65%
$\tilde{\lambda}$	<b>Dynamic</b>		
0.01	1.18%	0.57%	0.78%
0.1	1.89%	0.70%	0.99%
1	2.23%	0.44%	0.61%
10	2.31%	0.39%	0.49%

**Table 3** (CEP1) Fraction of instances with the lowest out-of-sample 2SP cost.

	$K = 1$	$K = 2$	$K = 5$
$\mathbb{E}[\omega \mathbf{x}]$	11.6%	0.15%	0.10%
MMD	0.0%	15.1%	11.7%
$\tilde{\lambda}$	<b>Static</b>		
0.01	29.8%	5.40%	2.10%
0.1	0.18%	4.85%	9.30%
1	0.00%	10.0%	13.7%
10	0.05%	12.6%	14.4%
$\tilde{\lambda}$	<b>Dynamic</b>		
0.01	55.7%	18.9%	15.5%
0.1	2.10%	9.15%	10.9%
1	0.40%	10.1%	9.03%
10	0.27%	13.8%	13.3%

### 4.3 Portfolio Optimization

**Problem Setting:** Next, we test CSG in a contextual portfolio optimization setting. In this application the trader wishes to select a portfolio  $\mathbf{y} \in \mathbb{R}_+^{n_{\text{assets}}}$  to balance risk and expectation of the portfolio return  $\omega^\top \mathbf{y}$  where  $\omega \in \mathbb{R}^{n_{\text{assets}}}$  denotes the asset-returns. For execution reasons, the portfolio must consist of some subset  $K_{\text{assets}} < n_{\text{assets}}$ . The trader wishes to use contextual information to make better decisions quickly. In this setting, the trader takes  $\mathbf{x} \in \mathbb{R}^{(n_{\text{assets}} + n_{\text{encoding}}) \times W}$  to be a panel of  $W$  past return observations for each of the  $n_{\text{assets}}$  assets, along with a representation of the 5-minute period within the 78 period trading session. The Conditional Value-at-Risk (CVaR) is the risk measure of choice. The reader is referred to Krokmal et al. [41] for more details regarding portfolio selection based on CVaR. The detailed formulation of the CVaR problem is relegated to Appendix C.3.1.

**Experimental Setup:** We consider a data-driven approach to set up the contextual environment. The trader assumes that the returns satisfy the following relationship:  $\omega = \Phi_\mu(\mathbf{x}) + \Phi_\sigma(\mathbf{x}) \odot \epsilon$ , where  $\Phi_\mu : \mathcal{X} \rightarrow \mathbb{R}^{n_{\text{assets}}}$  and  $\Phi_\sigma : \mathcal{X} \rightarrow \mathbb{R}_+^{n_{\text{assets}}}$  are models given to the trader by a statistical modeler to estimate the conditional mean  $\mathbb{E}[\omega|\mathbf{x}]$ , and conditional standard deviation  $\sqrt{\text{Var}[\omega|\mathbf{x}]}$  along with  $\epsilon$  denoting the errors which obey a uniform distribution supported on  $n^* = 1559$  points  $\{\epsilon^{(i)}\}_{i=1}^{n^*}$ , derived from a dataset of returns. The procedure defining  $\mathbb{P}_{\omega|\mathbf{x}}$  is fully described in Appendix C.3.2.

For a given contextual observation, the trader faces an instance of CVaR optimization defined on  $n^*$  scenarios. We aim to explore whether the CSG frameworks proposed in this work can enable the trader to directly generate a set of  $K$  scenarios from the context, which can then be solved more quickly than solving the problem on all  $n^*$  scenarios. We consider a training set and a validation set to evaluate our framework. The trained task-networks are evaluated on the validation set using  $\mathbb{P}_{\omega|\mathbf{x}}$  defined by  $\Phi_\mu$ ,  $\Phi_\sigma$  and  $\{\epsilon^{(i)}\}_{i=1}^{n^*}$ . This approach is sensible since our goal is to help the

trader solve their CVaR optimization with  $\mathbb{P}_{\omega|\mathbf{x}}$  defined as described above. Table 4 highlights the experiment parameters.

**Table 4** Summary of CVaR Experimental Parameters

Parameter	Value
Number of samples ( $n$ )	$\lfloor 0.8n^* + \frac{1}{2} \rfloor = 1247$
Number of out-of-sample instances ( $n_{\text{eval}}$ )	$n^* - \lfloor 0.8n^* + \frac{1}{2} \rfloor = 312$
Number of surrogate scenarios ( $K$ )	$\{1, 3, 5, 10, 20, 40\}$
MMD regularization ( $\lambda$ )	$\{80 * 2^i\}_{i=0}^7$

The resulting 2SP is mixed-binary in the first stage and is linear in the second stage; thus, there are no uniqueness guarantees. Furthermore, The task-net  $\mathbf{f}_\phi$  is parameterized by an LSTM network that outputs a  $n_{\text{assets}} \times K$  matrix.

**Results:** The CDF of the optimality gap for each method, by  $K$  and  $\lambda$  is relegated to Appendix C.3.3 for space considerations. Table 5 shows the median optimality gaps over the validation instances. Unlike CEP1, the value of stochastic solution is typically large, with the expected value solution exhibiting a median gap of 241%. Like the other experiments, the MMD approach produces solutions closer to optimal as  $K$  increases while underperforming the expected value solutions when  $K = 1$ .

**Table 5** (CVaR) Median optimality gaps on validation instances for various methods.

	$K = 1$	$K = 3$	$K = 5$	$K = 10$	$K = 20$	$K = 40$
$\mathbb{E}[\omega \mathbf{x}]$	241%	241%	241%	241%	241%	241%
MMD	483%	166%	122%	55.1%	18.7%	10.6%
$\lambda$	<b>Static</b>					
80	1.03e7%	486%	96.9%	79.0%	38.2%	118%
160	7.41e3%	120%	100%	84.9%	92.2%	25.7%
320	2.60e7%	106%	101%	45.7%	28.4%	11.9%
640	424%	98.4%	96.9%	93.8%	29.7%	10.9%
1280	456%	115%	77.1%	88.5%	15.8%	8.67%
2560	474%	182%	70.8%	32.5%	27.6%	12.4%
5120	486%	152%	94.1%	45.0%	19.5%	9.27%
10240	485%	164%	76.2%	33.6%	18.0%	17.5%
$\lambda$	<b>Dynamic</b>					
80	1.02e3%	296%	225%	94.8%	212%	62.8%
160	1.00e3%	310%	135%	93.5%	221%	54.1%
320	365%	172%	98.6%	60.8%	82.1%	20.2%
640	736%	154%	94.2%	28.6%	38.8%	11.6%
1280	433%	108%	91.2%	51.8%	24.2%	18.6%
2560	401%	89.5%	65.3%	39.6%	39.8%	7.55%
5120	439%	160%	66.2%	28.1%	14.4%	10.3%
10240	458%	148%	75.5%	29.9%	29.7%	5.07%



**Table 6** (CVaR) Fraction of instances with the lowest out-of-sample 2SP cost.

	$K = 1$	$K = 3$	$K = 5$	$K = 10$	$K = 20$	$K = 40$
$\mathbb{E}[\omega \mathbf{x}]$	74.4%	0.00%	0.00%	0.00%	0.00%	0.00%
MMD	0.32%	0.32%	0.00%	0.00%	30.8%	0.32%
$\lambda$	<b>Static</b>					
80	0.00%	0.00%	12.8%	6.09%	0.00%	0.00%
160	0.00%	8.65%	8.65%	4.81%	0.00%	0.00%
320	0.00%	13.1%	4.81%	0.00%	0.00%	4.81%
640	2.24%	14.7%	26.0%	0.00%	10.3%	29.5%
1280	4.17%	1.28%	0.00%	0.64%	13.8%	1.28%
2560	0.64%	0.00%	2.56%	0.32%	6.73%	0.00%
5120	0.32%	0.64%	0.00%	1.92%	0.00%	0.00%
10240	0.32%	0.96%	0.00%	20.2%	0.32%	0.00%
$\lambda$	<b>Dynamic</b>					
80	0.00%	0.00%	0.00%	0.00%	0.00%	0.00%
160	0.00%	0.00%	0.00%	0.00%	0.00%	0.00%
320	10.9%	0.00%	3.85%	0.32%	0.00%	5.13%
640	0.00%	6.73%	12.5%	19.9%	6.73%	3.21%
1280	2.88%	6.41%	1.28%	0.00%	0.00%	0.00%
2560	2.56%	44.2%	13.5%	0.00%	0.00%	3.53%
5120	1.28%	0.00%	13.1%	16.7%	31.4%	0.64%
10240	0.00%	2.88%	0.96%	29.2%	0.00%	51.6%

When  $K = 1$ , the CSG approaches do not outperform the expected value solution, although the static and dynamic methods tend to outperform the MMD approach for sufficiently large  $\lambda$ . The static and dynamic approaches also attain smaller optimality gaps than the MMD approach for  $K \geq 3$  and sufficiently large  $\lambda$ . For example, when  $K = 3$  and  $\lambda \geq 160$ , the static approach outperforms the MMD approach. Lastly, for any fixed  $K$ , the dynamic approach attains a smaller optimality gap than the static approach for some suitable value of  $\lambda$ . For instance, when  $K = 10$ , the dynamic approach attains a median gap of 28.1% when  $\lambda = 5120$ , whereas the static approach attains the static approach's best gap is 32.5% when  $\lambda = 2560$ . When  $K = 40$ , the static and dynamic approaches have median gaps less than 10.0%, whereas the MMD approach does not. Notably, the dynamic approach with  $(K, \lambda) = (40, 10240)$  can achieve a median gap of 5.07%.

Table 6 compares the performance of the different methods across  $K$  by showing the percentage of instances in which the particular method obtains the lowest out-of-sample 2SP cost (the columns sum to 100%). When  $K = 1$ , the expected value solution dominates; however, when  $K > 1$ , the expected value solution never obtains the lowest out-of-sample cost. Furthermore, the problem-driven approaches always out-perform when  $K > 1$ , since for every  $K$ , there is some  $\lambda$  such that the problem-driven approach wins most often. Unlike previous experiments, the task-based approaches offer more value than the MMD approach across all values of tested  $K$ .

#### 4.4 Multidimensional Newsvendor with Substitution

**Problem Setting:** Next, we test CSG in a contextual setting where the decision maker is tasked with solving a multidimensional newsvendor problem. We consider the version of the problem introduced by Narum et al. [20] and provide a brief overview. The Multidimensional Newsvendor with Substitution (MNV) is a production planning problem with a structure similar to (2), where production decisions regarding  $m$  products are made before uncertain demand  $\omega \in \mathbb{R}^m$  is realized. The primary distinction is that MNV considers multiple products and allows products to be substituted with each other. The original application by Vaagen et al. [42] considers fashion apparel where retailers offer substitutable products. The detailed formulation of the MNV problem is relegated to Appendix C.4.1.

**Experimental Setup:** Similar to newsvendor and CEP1, we consider randomly initialized neural networks to generate the conditional distribution  $\mathbb{P}_{\omega|\mathbf{x}}$  for context  $\mathbf{x}$ . The procedure used to define the underlying  $\mathbb{P}_{\omega|\mathbf{x}}$  is described in Appendix C.4.2. The process used to define  $\mathbb{P}_{\omega|\mathbf{x}}$  aims to capture the salient aspects of the product-demand distribution as pointed out by Vaagen et al. [42]. Table 7 highlights the experiment parameters.

**Table 7** Summary of MNV Experimental Parameters

Parameter	Value
Number of samples ( $n$ )	300
Number of out-of-sample instances ( $n_{\text{eval}}$ )	100
Number of surrogate scenarios ( $K$ )	{1, 3, 5, 10}
MMD regularization ( $\lambda$ )	$\{5 * 4^i\}_{i=0}^6$

The resulting MNV problem is a mixed-binary program (in both stages); thus, there are no uniqueness guarantees. Furthermore, the task-net  $\mathbf{f}_\phi$  is parameterized as a fully connected feedforward neural network with ReLU activation, mapping  $\mathbf{x}$  to  $\mathbb{R}_+^{m \times K}$ .

**Results:** The CDF of the optimality gap for each method, by  $K$  and  $\lambda$  is relegated to Appendix C.4.3 for space considerations. Table 8 shows the median optimality gaps over the validation instances. In the MNV setting, the value of stochastic solution is small, with the expected value solution exhibiting a median gap of 2.70%. The MMD approach produces solutions closer to optimal as  $K$  is increased. However, the MMD approach does not outperform for  $K > 1$  and outperforms the expected value solution when  $K = 10$ .

When  $K = 1$ , the CSG approaches underperform the expected value solution, although the static approach outperforms the MMD approach for sufficiently large  $\lambda \geq 80$ . When  $K = 3$ , the static and dynamic approaches underperform the MMD approach and perform similarly when  $\lambda = 20480$ . In the case,  $K = 5$ , the static approach ( $\lambda \geq 320$ ) attains smaller median gaps than the expected value and MMD approach, whereas the dynamic approach does not. In particular, the static method when  $(K, \lambda) \in \{(5, 5120), (5, 20480)\}$  attains smaller optimality gaps more frequently

than the expected value and MMD approaches (see Appendix C.4.3). Lastly, when  $K = 10$ , the static and dynamic approaches outperform the expected value approach, but only the static approach obtains similar performance on par with that of the MMD approach (when  $\lambda \in \{320, 5120\}$ ).

**Table 8** (MNV) Median optimality gaps on validation instances by method.

	$K = 1$	$K = 3$	$K = 5$	$K = 10$
$\mathbb{E}[\omega \mathbf{x}]$	2.70%	2.70%	2.70%	2.70%
MMD	3.81%	2.84%	2.82%	1.66%
$\lambda$	<b>Static</b>			
5	102%	37.5%	18.4%	13.4%
20	4.61%	9.78%	5.40%	2.60%
80	2.80%	4.86%	3.44%	1.93%
320	3.32%	3.17%	2.61%	1.75%
1280	3.67%	3.15%	2.65%	1.81%
5120	3.73%	2.89%	2.07%	1.73%
20480	3.72%	2.80%	2.19%	1.90%
$\lambda$	<b>Dynamic</b>			
5	74.7%	55.9%	29.8%	37.8%
20	8.69%	39.3%	23.2%	7.65%
80	3.26%	10.9%	5.73%	2.73%
320	3.70%	3.44%	3.12%	2.10%
1280	4.18%	3.76%	2.79%	2.16%
5120	4.26%	3.37%	2.89%	2.17%
20480	4.26%	2.83%	2.85%	2.01%

**Table 9** (MNV) Fraction of instances with the lowest out-of-sample 2SP cost.

	$K = 1$	$K = 3$	$K = 5$	$K = 10$
$\mathbb{E}[\omega \mathbf{x}]$	20.8%	13.8%	9.33%	10.0%
MMD	2.17%	11.7%	7.00%	9.50%
$\lambda$	<b>Static</b>			
5	2.17%	3.67%	0.67%	1.50%
20	12.5%	0.50%	8.00%	9.50%
80	11.5%	5.50%	6.50%	7.67%
320	2.00%	7.83%	6.17%	9.50%
1280	3.33%	8.17%	9.17%	7.00%
5120	2.00%	6.83%	10.0%	5.50%
20480	2.17%	10.7%	11.8%	7.33%
$\lambda$	<b>Dynamic</b>			
5	0.00%	0.00%	0.00%	0.83%
20	13.0%	0.00%	0.17%	2.00%
80	14.3%	0.17%	2.83%	5.83%
320	4.00%	7.50%	8.17%	7.17%
1280	4.50%	7.50%	7.33%	5.67%
5120	3.00%	7.33%	7.17%	5.17%
20480	2.50%	8.83%	5.17%	5.83%

Table 9 compares the performance of the different methods across  $K$  by showing the percentage of instances in which the particular method obtains the lowest out-of-sample 2SP cost (the columns sum to 100%). When  $K = 1$ , the expected value solution dominates; however, the static and dynamic approaches with  $\lambda \in \{20, 80\}$  are competitive. When  $K > 1$ , the expected value solution’s relative performance deteriorates by roughly a factor of 2. Furthermore, in the cases  $K > 1$ , the wins are split more evenly among the MMD, static, and dynamic approaches, where the static and dynamic approaches are heavily regularized.

Surprisingly, the dynamic approach fails to outperform the static approach (as one would expect that iteratively refining  $E_{\psi}$  would yield better results). In the MNV example,  $E_{\psi}$  was able to construct an accurate approximation on the dataset generated by the learned MMD task-net:  $\zeta_{1\dots K}^{(i)} = \hat{\mathbf{f}}_{\text{MMD}}(\mathbf{x}^{(i)})$ ,  $\ell_{\text{opt}}^{(i)} = \ell_{\text{opt}}(\zeta_{1\dots K}^{(i)}, \omega^{(i)})$ . However, the architecture for  $E_{\psi}$ , selected by random search with 20% hold out, did not generalize to the dataset generated in subsequent iterations of the dynamic approach. When one faces this situation, a sensible approach is to consider task-nets  $\mathbf{f}$  that produce  $\tilde{\zeta}_{1\dots K}^{(i)} = \mathbf{f}(\mathbf{x}^{(i)})$  that are close to  $\zeta_{1\dots K}^{(i)}$  with respect to MMD distance. Setting  $\lambda$  to a large value aims to achieve this, and indeed, we observe in Tables 8 and 9 that only

heavily regularized PCSG approaches achieve out-performance relative to the MMD approach.

## 4.5 Timing Analysis

This section explores the time trade-offs presented by the proposed methodologies. A time investment exists to train the task-net and loss-net used in the CSG approaches. However, once trained, the task-net can quickly generate solutions to 2SP by computing a forward pass through the task-net and solving ( $\zeta$ -SAA) on the resulting  $K$  surrogate scenarios. The following constitutes the relevant computation times:

- **MMD Training:** Time taken to train the task-net via DCSG.
- **Surrogate Solution Calculation:** Time taken to pass through the task network and compute an optimal solution to the ( $\zeta$ -SAA) problem for all  $n_{\text{eval}}$  contextual problems in the evaluation set.
- **2SP Solve:** Time taken to solve all  $n_{\text{eval}}$  contextual 2SPs in the evaluation set to optimality.
- **MMD Loss Evaluation:** Time taken to calculate the loss  $\ell_{\text{opt}}$  over the training sample  $S$ .
- **Loss-Net Training:** Time taken to train the loss network.
- **Static Training:** Time taken to train the task network via Static-PCSG.
- **Dynamic Training:** Time taken to train the task network via Dynamic-PCSG.

The computation times for the processes above are shown in Tables C1 and C2 for both the CVaR and MNV experiments, respectively, and are located in Appendix C.5. Tables C1 and C2 indicate that CSG’s trade-off between training time and quick surrogate solution evaluations can be worth it. For example, when  $K = 40$ , CSG can solve 312 CVaR instances in approximately 33 seconds using the dynamic approach with  $\lambda = 10240$ . The resulting solutions have a median optimality gap of 5.07%. Similar statements also hold for MNV. Although the CSG methods require additional time to train  $f$ , this time is incurred offline and is justified by repeatedly solving 2SPs in different contexts.

## 5 Conclusion

This work introduces CSG, a framework for solving 2SPs in contextual settings. In time-sensitive applications, here-and-now decisions are required that consider the distribution of uncertainty conditioned on the available context. It is desirable to obtain solutions to contextual 2SPs efficiently. In this aim, CSG proposes learning a mapping from context to a set of  $K$  scenarios that can then be used to solve the deterministic equivalent of the 2SP defined on the  $K$  scenarios. CSG leverages contextual information to learn task-mappings that produce high-quality decisions while reducing the computational burden of solving large-scale stochastic programs repeatedly.

Motivated by distributional approaches to scenario generation, we propose a distributional approach that leverages the MMD distance to create task mappings that remain close to the true conditional distribution across contexts. This method only requires joint samples, typically available in historical data, and does not need direct

access to the true conditional distributions. Furthermore, we propose a problem-driven approach based on a bi-level scenario generation problem that addresses non-unique solutions and sparse gradients. Non-unique solutions are addressed by introducing an optimistic loss function that is easily computable for a large class of 2SPs. Furthermore, we mitigate the issue of sparse gradients by using a neural network to approximate the proposed problem-driven loss. We subsequently use the trained network along with MMD regularization to guide the gradient-based search for the task network. Lastly, we propose a dynamic approach that extends the static approach by iteratively refining the loss-net and task-net in an alternating fashion. We observe that the dynamic approach can improve the performance of the static approach if the loss-net can sufficiently approximate the problem-driven loss.

A diverse array of contextual problem settings is employed to demonstrate the framework’s effectiveness and illustrate its flexibility. We show that the proposed problem-driven methods rely critically on MMD regularization to produce high-quality task nets. Furthermore, we observe that the proposed methodology can unlock the value of stochastic solutions and can compute high-quality solutions in the considered problem settings. Additionally, the offline cost of training the models required for CSG is justified by the time savings in computing solutions to contextual 2SPs.

Future work could explore the application and impacts of different distributional distance measures. Furthermore, understanding finite sample learning bounds and the generalization/stability properties of the proposed methodologies is of interest. For instance, the MMD distance is rooted in kernel methods that have rich generalization theory [25]. Lastly, problem-specific extensions and structured architectures could reveal new insights in the field of contextual optimization.

## **Acknowledgements**

The authors received financial support from the a joint International Doctoral Cluster between the KAIST and the University of Toronto, Department of Mechanical and Industrial Engineering.

## **Declarations**

### **Funding**

Financial support was provided by NSERC Grant 455963 for David Islip and Roy H. Kwon.

### **Conflict of interest**

The authors have no relevant financial or non-financial interests to disclose.

### **Data availability**

All data used in the experiments is either simulated (and accessible in the Appendix) or available via the Tiingo data service (<https://www.tiingo.com/>).

## Author contribution

- David Islip: Writing - review & editing, Writing - original draft, Validation, Software, Methodology, Formal analysis, Conceptualization.
- Roy H. Kwon: Writing - review & editing, Writing - original draft, Supervision, Resources, Project administration, Funding acquisition, Conceptualization.
- Sanghyeon Bae: Writing - review & editing, Methodology, Formal analysis, Conceptualization
- Woo Chang Kim: Writing - review & editing, Supervision, Resources, Project administration, Funding acquisition, Conceptualization.

## Appendix A Comparing Conditional Distributions

In general, MMD distances differ from Wasserstein distances in several key regards. Computing Wasserstein metrics between two samples of size  $n$  requires  $O(\log(n)n^3)$  operations, whereas MMD requires  $n^2$  operations [43]. Additionally, Wasserstein metrics have dimension-dependent sample complexity and require more samples in higher dimensional settings to bound the gap between the sampled distance and the true distance [44]. Wasserstein also suffers from biased sample gradients [45] unlike MMD. However, MMD induces a geometry on the space of probability measures that does not respect the distance metric on the underlying space. Feydy et al. [46] use Sinkhorn divergence: an entropic regularization of the Wasserstein distance with bias removed. They show that the Sinkhorn divergence interpolates between Wasserstein and MMD of the Laplacian RKHS based on the amount of regularization. The interpolation property also applies to complexities, with Sinkhorn achieving  $O(n^2)$  and  $O(1/\sqrt{n})$  computational and sample complexity, respectively [44]. However, computing Sinkhorn divergence takes approximately 20-50 times as long as computing MMD [46].

Ren et al. [47] and Park and Muandet [48] consider conditional versions of the MMD metric that only require joint sampling access, however, Huang et al. [27] points out that optimizing these metrics via batched gradients requires matrix inversions that scale with the batch size. Some authors consider  $d_{\mathcal{F}_{\text{MMD}}}^2(\mathbb{P}_{\mathbf{x},\omega}, \mathbb{P}_{\mathbf{x},\eta})$  to infer a relationship between  $\mathbb{P}_{\omega|\mathbf{x}}$  and  $\mathbb{P}_{\eta|\mathbf{x}}$ . For instance, Huang et al. [27] (Theorem 6) claim, under suitable assumptions (measurability, boundedness in expectation and characteristic kernels) that  $d_{\mathcal{F}_{\text{MMD}}}^2(\mathbb{P}_{\mathbf{x},\omega}, \mathbb{P}_{\mathbf{x},\eta}) = 0 \iff \mathbb{P}_{\omega|\mathbf{x}} = \mathbb{P}_{\eta|\mathbf{x}}$  almost everywhere according to  $\mathbb{P}_{\mathbf{x}}$ . In the case of the energy distance, Hagemann et al. [49] bounds  $\mathbb{E}_{\mathbf{x} \sim \mathbb{P}_{\mathbf{x}}} [d_{\mathcal{F}_{\text{MMD}}}^2(\mathbb{P}_{\omega|\mathbf{x}}, \mathbb{P}_{\eta|\mathbf{x}})]$  by  $d_{\mathcal{F}_{\text{MMD}}}^2(\mathbb{P}_{\mathbf{x},\omega}, \mathbb{P}_{\mathbf{x},\eta})^{\frac{1}{4(1+p+d)}}$  under regularity and compactness assumptions. Chemseddine et al. [50] show the opposite relationship holds for the 1-Wasserstein metric and consequently introduce a Wasserstein distance of order  $q$ , conditioned on  $\mathbf{x}$ , denoted by  $d_{q,\mathbf{x}}$  that satisfies  $\mathbb{E}_{\mathbf{x} \sim \mathbb{P}_{\mathbf{x}}} [d_{q,\mathbf{x}}^q(\mathbb{P}_{\omega|\mathbf{x}}, \mathbb{P}_{\eta|\mathbf{x}})] = d_{q,\mathbf{x}}^q(\mathbb{P}_{\mathbf{x},\omega}, \mathbb{P}_{\mathbf{x},\eta})$ , where  $d_q^q(\cdot, \cdot)$  denotes the  $q$ -Wasserstein distance raised to the power  $q$ . In practice, Chemseddine et al. [50] implement their conditional distance by penalizing transport cost associated with  $\mathbf{x}$  and use Feydy et al. [46]’s debiased Sinkhorn approach to compute the distance.

## Appendix B Proof of Proposition 2

In this section, we provide proof of Proposition 2. The proof largely relies on Proposition 1 due to Tabaghi and Wang [35]. First, we introduce some notation, followed by Proposition 1 by Tabaghi and Wang [35] and the proof of Proposition 2.

### Notation

A multiset is a pair  $(U, \nu)$  where  $U$  denotes a set of objects and  $\nu$  maps  $U$  to the non-negative integers, where  $\nu(u)$  represents the cardinality of object  $u \in U$ . Multisets are denoted by double brackets  $\{\{\}\}$ . For example, the multiset  $\{\{3, 3, 4\}\}$  has three elements with  $\nu(3) = 2$  and  $\nu(4) = 1$ . For any domain  $\Omega$ , a multiset  $U$  such that  $U \subseteq \Omega$  means that the elements of  $U$  are in  $\Omega$ . The cardinality of  $U$ , denoted by  $|U|$  is the number of elements in  $U$ , counting repetitions, e.g.  $|\{\{3, 3, 4\}\}| = 3$ . For some  $N$  in the positive integers  $\mathbb{N}$  and domain  $\Omega$ , the following sets are introduced

$$\mathbb{U}_{\Omega, N} = \{\text{multiset } U \subseteq \Omega : |U| = N\} \text{ and } \mathbb{U}_{\Omega, [N]} = \{\text{multiset } U \subseteq \Omega : |U| \in [N]\}.$$

### Tabaghi and Wang [35]’s Proposition 1

Tabaghi and Wang [35] prove the following proposition regarding functions of multisets, which we repeat here for the reader’s convenience.

**Proposition 3** (Proposition 1 from (Tabaghi and Wang 2024)).

A (continuous) multiset function  $f : \mathbb{U}_{\Omega, [N_1]} \times \mathbb{U}_{\Omega, [N_2]} \rightarrow \text{codom}(f)$ , where  $\Omega$  is a compact subset of  $\mathbb{R}^p$ , is (continuously) sum-decomposable via  $\mathbb{R}^{\binom{N+p}{p}-1} \times \mathbb{R}^{\binom{N+p}{p}-1}$ , that is,

$$f(U, U') = \tilde{\rho} \left( \sum_{x \in U} \tau(x), \sum_{x' \in U'} \tau(x') \right) \quad \forall U \in \mathbb{U}_{\Omega, [N_1]}, U' \in \mathbb{U}_{\Omega, [N_2]}$$

where continuous  $\tau : \mathbb{R}^p \rightarrow \mathbb{R}^{\binom{N+p}{p}-1}$ ,  $N = \max\{N_1, N_2\}$  and (continuous)  $\tilde{\rho} : \mathbb{R}^{\binom{N+p}{p}-1} \times \mathbb{R}^{\binom{N+p}{p}-1} \rightarrow \text{codom}(\tilde{\rho})$ , and  $\text{codom}(f) \subset \text{codom}(\tilde{\rho})$ .

### Proof of Proposition 2

*Proof.* First, fix a value of  $K \in \mathbb{N}$ . We can identify  $\ell_{\text{opt}}$  as a multiset function. Since the value  $\ell_{\text{opt}}(\zeta_{1 \dots K'}, \omega)$  does not depend on the order of the  $K' \in \mathbb{N}$  scenarios  $\zeta_{1 \dots K'}$ , we can define the multisets  $U_{\zeta_{1 \dots K'}} = \{\{\zeta_k\}_{k=1}^{K'}\} \in \mathbb{U}_{\Omega, K'}$  and  $U_\omega = \{\{\omega\}\} \in \mathbb{U}_{\Omega, 1}$  and define  $\ell'_{\text{opt}} : \mathbb{U}_{\Omega, [K']} \times \mathbb{U}_{\Omega, 1} \rightarrow \text{codom}(\ell_{\text{opt}})$  such that

$$\ell'_{\text{opt}}(U_{\zeta_{1 \dots K'}}, U_\omega) = \ell_{\text{opt}}(\zeta_{1 \dots K'}, \omega) \quad \forall \zeta_{1 \dots K'} \in \Omega^{K'}, \omega \in \Omega, \forall K' \in [K].$$

The value of  $\ell'_{\text{opt}}(U_{\zeta_{1\dots K'}}, U_{\omega})$  is calculated by solving ( $\zeta$ -SAA) on the multiset of scenarios  $U_{\zeta_{1\dots K'}}$  and optimistically evaluating the resulting solutions on the singleton-multiset  $U_{\omega}$ . Applying Proposition 1 from [35], to  $\ell'_{\text{opt}}$  implies

$$\ell'_{\text{opt}}(U, U') = \tilde{\rho}\left(\sum_{u \in U} \tau(u), \sum_{u' \in U'} \tau(u')\right) \quad \forall U \in \mathbb{U}_{\Omega, [K]}, U' \in \mathbb{U}_{\Omega, [1]}, \quad (\text{B1})$$

where  $N = \max\{K, 1\} = K$ , continuous  $\tau : \mathbb{R}^p \rightarrow \mathbb{R}^{\binom{K+p}{p}-1}$ , (continuous)  $\tilde{\rho} : \mathbb{R}^{\binom{K+p}{p}-1} \times \mathbb{R}^{\binom{K+p}{p}-1} \rightarrow \text{codom}(\tilde{\rho})$ , and  $\text{codom}(\ell'_{\text{opt}}) \subset \text{codom}(\tilde{\rho})$ . Since (B1) holds for all  $U \in \mathbb{U}_{\Omega, [K]}$ , it also holds for all  $U \in \mathbb{U}_{\Omega, K}$ , implying

$$\begin{aligned} \ell_{\text{opt}}(\zeta_{1\dots K}, \omega) &= \tilde{\rho}\left(\sum_{\zeta \in U_{\zeta_{1\dots K}}} \tau(\zeta), \sum_{\omega \in U_{\omega}} \tau(\omega)\right) \\ &= \tilde{\rho}\left(\sum_{k=1}^K \tau(\zeta_k), \tau(\omega)\right) \quad \forall \zeta_{1\dots K} \in \Omega^K, \omega \in \Omega. \end{aligned}$$

Lastly, letting  $\rho : \mathbb{R}^{\binom{K+p}{p}-1} \times \mathbb{R}^{\binom{K+p}{p}-1} \rightarrow \text{codom}(\tilde{\rho})$  be defined such that

$$\rho(\hat{\zeta}, \hat{\omega}) = \tilde{\rho}(K\hat{\zeta}, \hat{\omega}) \quad \forall \hat{\zeta} \in \mathbb{R}^{\binom{K+p}{p}-1}, \hat{\omega} \in \mathbb{R}^{\binom{K+p}{p}-1},$$

yields the desired result.  $\square$

## Appendix C Experimental Information

### C.1 Experimental Tools

The mathematical programming models are implemented in Python 3.7 and solved using Gurobi 11.0 on Google Colab equipped with an Intel(R) Xeon(R) CPU 2.20GHz, 51 gigabytes of random access memory (RAM) and a Tesla T4 GPU. All neural networks are trained using skorch [51].

### C.2 CEP1 Experimental Supplement

#### C.2.1 CEP1 Formulation

Based on the CEP1 problem description, the decision-maker wishes to solve

$$\begin{aligned} \min_{\mathbf{y}} \quad & \mathbf{c}^T \mathbf{y}_{\text{cap}} + \mathbb{E}_{\omega \sim \mathbb{P}_{\omega|\mathbf{a}}} [Q(\mathbf{y}_{\text{op}}, \omega)] & (\text{CEP1}) \\ \text{s.t.} \quad & -y_{\text{cap},j} + y_{\text{op},j} \leq h_j & \forall j \in [n_{\text{machines}}] \\ & \mathbf{t}^T \mathbf{y}_{\text{op}} \leq T \\ & \mathbf{0} \leq \mathbf{y}_{\text{cap}}, \mathbf{0} \leq \mathbf{y}_{\text{op}} \leq \mathbf{u}, \end{aligned}$$



where  $\mathbf{y}_{\text{cap}}$  and  $\mathbf{y}_{\text{op}}$  denote the hours of added capacity and total operation of the machines, respectively.  $\mathbf{c} \in \mathbb{R}_+^{n_{\text{machines}}}$  denotes the capacity cost vector,  $\mathbf{h} \in \mathbb{R}_+^{n_{\text{machines}}}$  denotes the baseline capacities of the machines,  $\mathbf{t} \in \mathbb{R}_+^{n_{\text{machines}}}$  is the maintenance requirements incurred per hour for all the machines,  $T$  is the total maintenance limit, and  $\mathbf{u} \in \mathbb{R}_+^{n_{\text{machines}}}$  denotes the upper bounds on utilization for each machine. The recourse cost is given by

$$\begin{aligned}
Q(\mathbf{y}_{\text{op}}, \omega) = \min_{\mathbf{z}, \mathbf{s}} \quad & \sum_{i=1}^m \sum_{j=1}^{n_{\text{machines}}} g_{ij} z_{ij} + \sum_{i=1}^m p_i s_i & (\text{CEP1-Stage II}) \\
\text{s.t.} \quad & \sum_{j=1}^{n_{\text{machines}}} a_{ij} z_{ij} + s_i \geq \omega_i & \forall i \in [m] \\
& \sum_{i=1}^m z_{ij} \leq y_{\text{op},j} & \forall j \in [n_{\text{machines}}] \\
& z_{ij} \geq 0 & \forall i \in [m], j \in [n_{\text{machines}}] \\
& s_i \geq 0 & \forall i \in [m],
\end{aligned}$$

where  $z_{ij}$  and  $s_i$  denote the hours producing part  $i$  on machine  $j$  and the production shortfall of part  $i$  respectively. The uncertain demand for part  $i$  is  $\omega_i$ . Machine  $j$  produces part  $i$  at a rate of  $a_{ij} \geq 0$  with an hourly cost of  $g_{ij} \geq 0$ . Production shortfalls incur a penalty of  $p_i \geq 0$ . We use the same deterministic problem data as defined by [5] with  $n_{\text{machines}} = 4$  and  $m = 3$ . The static data below is used to define the CEP1 instance considered in the manuscript.

$$n = 4, \quad m = 3, \quad T = 100$$

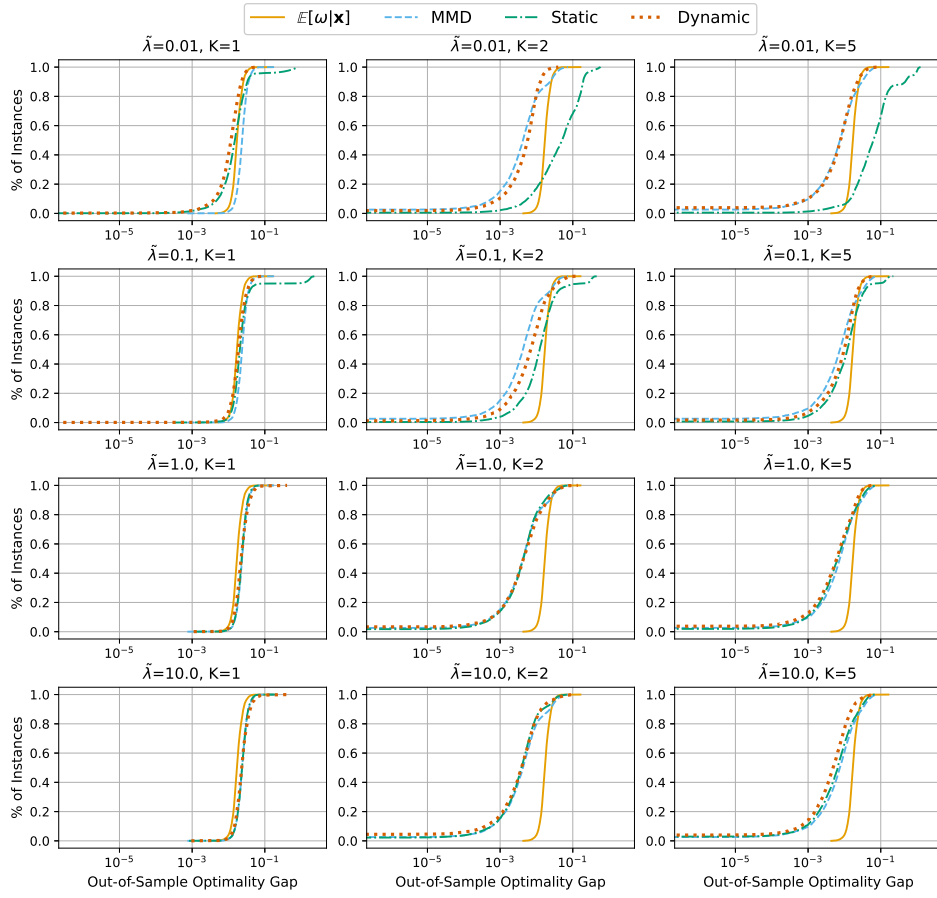
$$\begin{aligned}
\mathbf{c} &= (2.5, 3.75, 5.0, 3.0), & \mathbf{t} &= (0.08, 0.04, 0.03, 0.01) \\
\mathbf{h} &= (500, 500, 500, 500), & \mathbf{u} &= (2000, 2000, 3000, 3000) \\
\mathbf{p} &= (400, 400, 400) \\
[a_{ij}] &= \begin{bmatrix} 0.6 & 0.6 & 0.9 & 0.8 \\ 0.1 & 0.9 & 0.6 & 0.8 \\ 2.6 & 3.4 & 3.4 & 0.9 \end{bmatrix}, & [q_{ij}] &= \begin{bmatrix} 1.5 & 2.3 & 2.0 & 3.6 \\ 0.05 & 0.2 & 0.5 & 0.8 \end{bmatrix}
\end{aligned}$$

### C.2.2 CEP1 Stochastic Modelling

Higle and Sen [5] originally consider  $\omega_i, i \in \{1, 2, 3\}$  as an iid discrete random variable with  $\omega_i \in \{0, 600, 1200, 1800, 2400, 3000\}$  being equally likely. We construct our contextual setting similarly. The contextual information  $\mathbf{x}$  is distributed according to a four-dimensional normal distribution  $N(\mathbf{0}, \mathbf{I})$ . A neural network  $\mathbf{f}_{\text{Random}} : \mathcal{X} \rightarrow \mathbb{R}^{6 \times m}$  is randomly initialized. For part  $i$ , the  $i$ th column of  $\mathbf{f}_{\text{Random}}(\mathbf{x})$  corresponds to the 6 points defining the support of  $\omega_i$ . Since each demand  $\omega_i$  is supported on 6 points, there are 216 possibilities defining the demand distribution conditional on the context. Scaling is applied to the outputs from  $\mathbf{f}_{\text{Random}}$  such that the demands expectation and standard deviation are 1500 and 1024.7, respectively. Any negative demand values are clipped to 0. This process defines  $\mathbb{P}_{\omega|\mathbf{x}}$ .

### C.2.3 CEP1 Optimality Gap CDFs

Fig. C1 Out of sample optimality gaps for the contextual CEP1 problem.



## C.3 CVaR Experimental Supplement

### C.3.1 CVaR Formulation

We consider a trader who wishes to balance the trade-off between risk and expected return. CVaR is used as the risk measure, and we employ the formulations introduced by Krokmal et al. [41] to model the trader’s problem. The trader wishes to solve

$$\begin{aligned} \min_{\mathbf{y}, \gamma, \mathbf{t}} \quad & -\mathbb{E}_{\omega \sim \mathbb{P}_{\omega|\mathbf{x}}}[\omega]^\top \mathbf{y} + \lambda_{\text{risk}} \left( \gamma + \frac{1}{1-\alpha} \mathbb{E}_{\omega \sim \mathbb{P}_{\omega|\mathbf{x}}} [Q(\mathbf{y}, \gamma, \omega)] \right) & (\text{CVaR}) \\ \text{s.t.} \quad & \mathbf{1}^\top \mathbf{y} = 1, \\ & y_i \leq t_i \quad \forall i \in [n_{\text{assets}}], \\ & \mathbf{1}^\top \mathbf{t} \leq K_{\text{assets}}, \\ & \mathbf{y} \in \mathbb{R}_+^{n_{\text{assets}}}, \quad \gamma \in \mathbb{R}, \quad \mathbf{t} \in \{0, 1\}^{n_{\text{assets}}}, \end{aligned}$$

where  $\mathbf{y}$ ,  $\gamma$ , and  $\omega$  represent the selected portfolio, a placeholder variable that at optimality equals the portfolio’s value at risk (VaR) according to  $\mathbb{P}_{\omega|\mathbf{x}}$ , and the binary indicator variables that model  $w_i = 0 \implies y_i = 0, \forall i \in [n_{\text{assets}}]$ , respectively. The variables  $\mathbf{y}$ ,  $\gamma$ , and  $\omega$  constitute the first-stage decisions. The relative risk aversion and VaR confidence level are denoted by  $\lambda_{\text{risk}} > 0$  and  $\alpha \in (0, 1)$ , respectively. The  $n_{\text{assets}}$  random returns for each asset are represented by  $\omega$ . Lastly, the recourse cost is given by

$$\begin{aligned} Q(\mathbf{y}, \gamma, \omega) = \min_z \quad & z & (\text{CVaR}) \\ \text{s.t.} \quad & z \geq -\omega^\top \mathbf{y} - \gamma \\ & z \geq 0, \end{aligned}$$

where  $z$  is a variable that models the portfolio loss exceeding the value at risk. We consider the following instance parameters  $\lambda_{\text{risk}} = 10$ ,  $n_{\text{assets}} = 10$ ,  $K_{\text{assets}} = 5$ , and  $\alpha = 0.9$ .

### C.3.2 CVaR Stochastic Modelling

A data-driven approach is considered to set up the contextual environment. The decision-maker limits the selection to tickers in the S&P 500 as of December 29, 2023, and chooses the  $n_{\text{assets}}$  tickers with the smallest traded volumes as their asset universe. They desire the ability to be able to obtain portfolios that are of high quality according to (CVaR) every 5 minutes for hedging purposes. The context window  $W$  is set to 78 periods (a full trading session). Furthermore, as discussed in the text, the trader assumes that the returns satisfy the following relationship

$$\omega = \Phi_\mu(\mathbf{x}) + \Phi_\sigma(\mathbf{x}) \odot \epsilon \tag{C2}$$

where  $\Phi_\mu : \mathcal{X} \rightarrow \mathbb{R}^{n_{\text{assets}}}$  and  $\Phi_\sigma : \mathcal{X} \rightarrow \mathbb{R}_+^{n_{\text{assets}}}$  are models given to the trader by a statistical modeler to estimate the conditional mean  $\mathbb{E}[\omega|\mathbf{x}]$ , and conditional standard

deviation  $\sqrt{\text{Var}[\omega|\mathbf{x}]}$  along with  $\boldsymbol{\epsilon}$  denoting the random errors. There is a large dataset  $S^* = \{\mathbf{x}^{(i)}, \omega^{(i)}\}_{i=1}^{n^*}$  of size  $n^*$  used to produce  $\Phi_{\boldsymbol{\mu}}$  and  $\Phi_{\boldsymbol{\sigma}}$ . Similar to Deng and Sen [52] and Ban et al. [8], the residuals obtained from the trained models define the conditional distribution. That is,  $\boldsymbol{\epsilon}$  is assumed to be uniformly distributed over  $\{\boldsymbol{\epsilon}^{(i)}\}_{i=1}^{n^*}$  where

$$\boldsymbol{\epsilon}^{(i)} = \left( \omega^{(i)} - \Phi_{\boldsymbol{\mu}}(\mathbf{x}^{(i)}) \right) \odot \begin{pmatrix} 1/\Phi_{\sigma,1}(\mathbf{x}^{(i)}) \\ 1/\Phi_{\sigma,2}(\mathbf{x}^{(i)}) \\ \vdots \\ 1/\Phi_{\sigma,n_{\text{assets}}}(\mathbf{x}^{(i)}) \end{pmatrix}, \quad \forall i \in [n^*]. \quad (\text{C3})$$

Thus, the trader aims to solve (CVaR) with  $\mathbb{P}_{\omega|\mathbf{x}}$  defined by (C2) and  $\boldsymbol{\epsilon} \sim \text{uniform}\{\boldsymbol{\epsilon}^{(i)}\}_{i=1}^{n^*}$ .

A dataset of prices consisting of 21 trading periods is gathered for each ticker via the IEX endpoint available via the Tiingo API, resulting in 1638 returns  $\mathbf{r}^{(j)} \in \mathbb{R}^{n_{\text{assets}}}$ ,  $j = 1, \dots, 1638$ . The sample  $S^*$  used to train  $\Phi_{\boldsymbol{\mu}}$  and  $\Phi_{\boldsymbol{\sigma}}$  is formed as follows

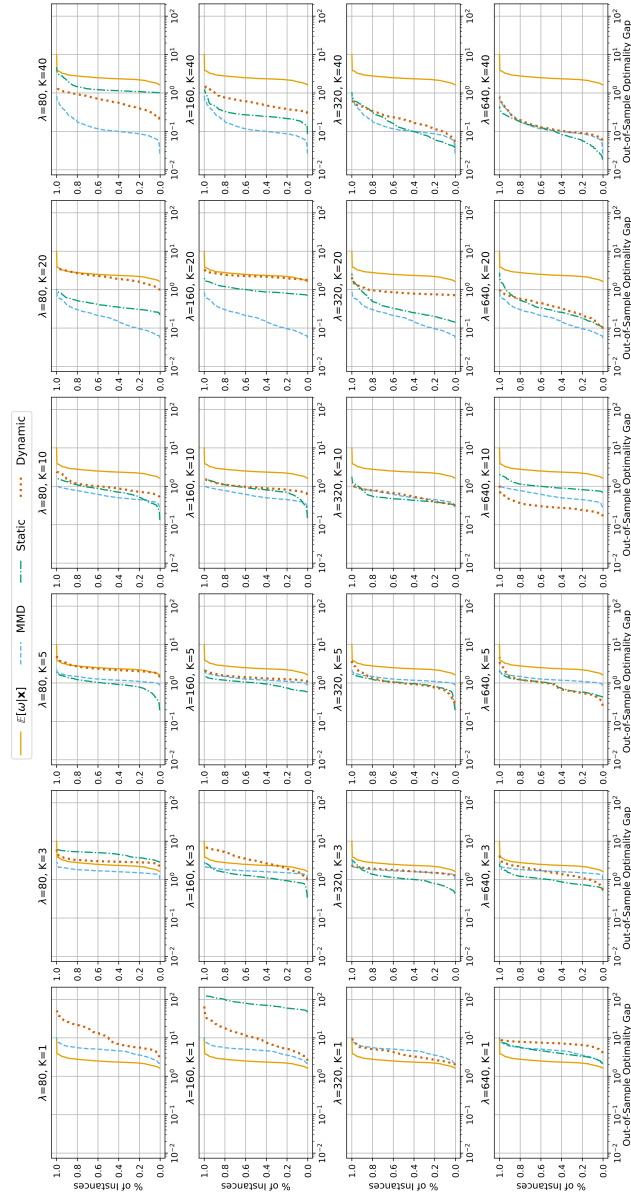
$$\mathbf{x}^{(i)} = \begin{pmatrix} \mathbf{r}^{(i)} & \dots & \mathbf{r}^{(i+W)} \\ (\text{PE}_{i\dots i+W}^{(1)})^\top \\ \vdots \\ (\text{PE}_{i\dots i+W}^{(n_{\text{encoding}})})^\top \end{pmatrix} \text{ and } \omega^{(i)} = \mathbf{r}^{(i+W+1)}, \quad i = 1, \dots, n^* := 1559,$$

where  $\text{PE}_{i\dots i+W}^{(j)} \in \mathbb{R}^W$  is the  $j$ th sinusoidal positional encoding of the period associated with indices  $i, \dots, W + i$  (the period of the  $i$ th datum is given by  $i$  modulo 78) [53]. We design  $\Phi_{\boldsymbol{\mu}}$  and  $\Phi_{\boldsymbol{\sigma}}$  such that the resulting distribution can generate the dataset  $S^*$  as a sample. Specifically,  $\Phi_{\boldsymbol{\mu}}$  and  $\Phi_{\boldsymbol{\sigma}}$  are parameterized by long short-term memory (LSTM) neural networks. The parameters of these networks are selected via random search, using a 20% holdout for validation.

The networks  $\Phi_{\boldsymbol{\mu}}$  and  $\Phi_{\boldsymbol{\sigma}}$  are fit in a two-step training procedure. First we train  $\Phi_{\boldsymbol{\mu}}$  by optimizing  $\frac{1}{n} \sum_{i=1}^n \|\hat{\mathbf{r}}_i - \Phi_{\boldsymbol{\mu}}(\mathbf{x}_i)\|_1$ . Then the vectors of residuals  $\hat{\boldsymbol{\eta}}_i = |\hat{\mathbf{r}}_i - \hat{\Phi}_{\boldsymbol{\mu}}(\mathbf{x}_i)|$  are formed and  $\Phi_{\boldsymbol{\sigma}}$  is obtained by minimizing  $\frac{1}{n} \sum_{i=1}^n \|\hat{\boldsymbol{\eta}}_i - \Phi_{\boldsymbol{\sigma}}(\mathbf{x}_i)\|_1$ . Lastly equation (C3) yields  $\{\boldsymbol{\epsilon}^{(i)}\}_{i=1}^{n^*}$ .

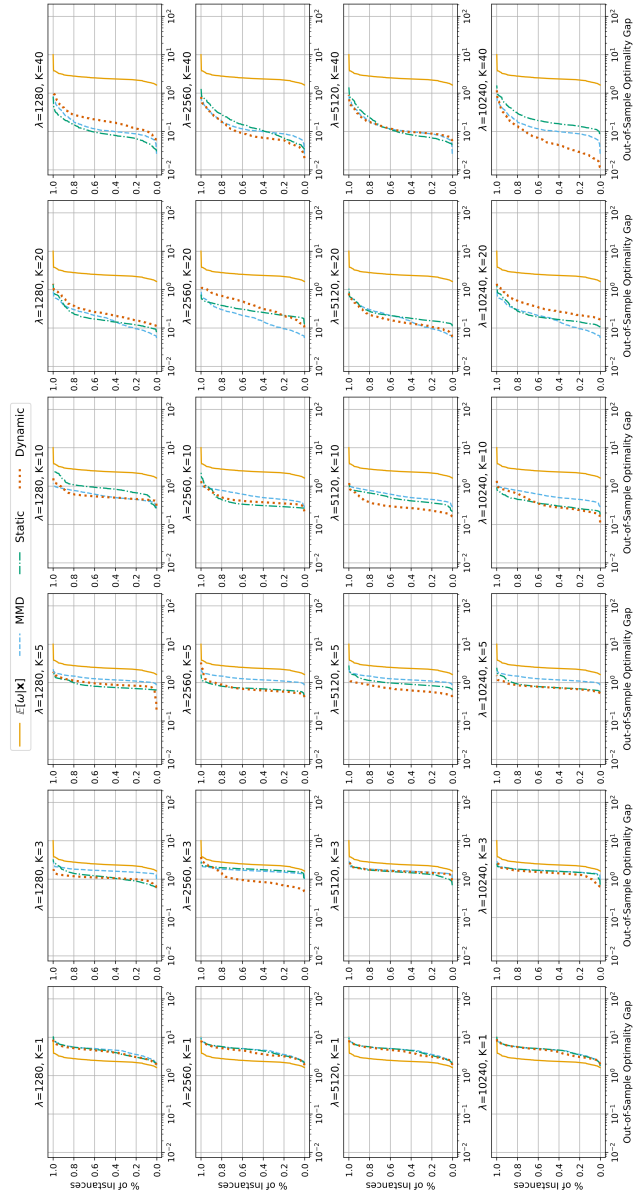
### C.3.3 CVaR Optimality Gap CDFs

Fig. C2 Out of sample optimality gaps for the contextual CVaR problem



Note. Figure continued on next page

Fig. C3 Out of sample optimality gaps for the contextual CVaR problem



## C.4 MNV Experimental Supplement

### C.4.1 MNV Formulation

This section presents the MNV problem as considered by Narum et al. [20]. There are  $m$  products available for production. The decision maker wishes to select a production plan to produce at most  $P$  items while respecting the overall production capacity  $C$ . They wish to solve

$$\begin{aligned}
\max_{\mathbf{y}, \mathbf{t}} \quad & \mathbb{E}_{\omega \sim \mathbb{P}_{\omega} | \mathbf{x}} [Q(\mathbf{y}, \omega)] - \sum_{i=1}^m c_i y_i & (\text{MNV}) \\
\text{s.t.} \quad & \sum_{i=1}^m y_i \leq C \\
& \sum_{i=1}^m t_i \leq P \\
& y_i \leq M t_i \quad \forall i \in [m] \\
& \mathbf{y} \in \mathbb{R}_+^m, \mathbf{t} \in \{0, 1\}^m,
\end{aligned}$$

where  $y_i$  represents the amount of product  $i$  produced,  $t_i$  represents the binary decision indicating that product  $i$  is eligible for production, and  $c_i$  is the product  $i$  production cost.

The recourse profit is the total of the salvage values and the sales values, which come from both direct sales and customer-driven substitutions. The recourse profit is given by

$$\begin{aligned}
Q(\mathbf{y}, \omega) = \max_{\mathbf{s}, \mathbf{z}, \bar{\mathbf{z}}, \mathbf{w}, \hat{\mathbf{z}}} \quad & \sum_{i=1}^m (v_i s_i + v_i \bar{z}_i + g_i w_i) & (\text{MNV-Stage II}) \\
\text{s.t.} \quad & s_i + \sum_{j \in [m]: j \neq i} z_{ji} \leq \omega_i \quad \forall i \in [m] \\
& z_{ij} \leq \alpha_{ij} (\omega_j - s_j) \quad \forall i \in [m], j \in [m], i \neq j \\
& \bar{z}_i = \sum_{j \in [m]: j \neq i} z_{ij} \quad \forall i \in [m] \\
& M(\hat{z}_j - 1) \leq s_j - y_j \quad \forall j \in [m] \\
& z_{ij} \leq M \hat{z}_j \quad \forall i \in [m], j \in [m] \\
& w_i = y_i - (s_i + \bar{z}_i) \quad \forall i \in [m] \\
& \hat{z}_{ij} \in \{0, 1\} \quad \forall i \in [m], j \in [m], i \neq j \\
& \mathbf{s}, \mathbf{z}, \bar{\mathbf{z}}, \mathbf{w} \in \mathbb{R}_+^m,
\end{aligned}$$

where  $s_i$  represents the sales of product  $i$ ,  $z_{ij}$  is the substitution sale amount of item  $i$  to satisfy demand for item  $j$ ,  $\bar{z}_i$  and the total amount of item  $i$  substituted,  $w_i$

represents unsold inventory that is salvaged, and  $\hat{z}_j$  is a binary variable indicating whether to start substitution sales satisfying demand for item  $j$ .

In the objective, parameters  $v_i$  and  $g_i$  denote the sales price and salvage value of item  $i$ . The substitution rate  $\alpha_{ij}$  average probability that item  $j$  can be replaced by item  $i$ .  $\alpha_{ij}$  is not necessarily symmetric, e.g., pink t-shirts can be substituted with white t-shirts more often than white shirts can with pink. The big- $M$ s are set to be the capacity  $C$ . Lastly,  $\omega \in \mathbb{R}_+^m$  denotes the uncertain demand for the  $m$  products. We consider a setting with  $m = 6$  potential products. The static data below is used to define the MNV instance considered in the manuscript.

$$\mathbf{v} = (46.111, 44.691, 46.448, 48.406, 44.476, 44.476),$$

$$\mathbf{c} = (18.980, 25.618, 24.163, 26.217, 17.974, 26.418),$$

$$\mathbf{g} = (9.830, 5.094, 5.067, 5.293, 5.723, 7.292)$$

$$[\gamma_{ij}] = \begin{bmatrix} - & 0.087 & 0.184 & 0.042 & 0.088 & 0.110 \\ 0.137 & - & 0.060 & 0.154 & 0.178 & 0.014 \\ 0.182 & 0.051 & - & 0.285 & 0.290 & 0.243 \\ 0.091 & 0.029 & 0.205 & - & 0.037 & 0.149 \\ 0.010 & 0.273 & 0.078 & 0.199 & - & 0.156 \\ 0.164 & 0.055 & 0.291 & 0.233 & 0.282 & - \end{bmatrix},$$

along with the constants  $C = 70$  and  $P = 3$ .

## C.4.2 MNV Stochastic Modelling

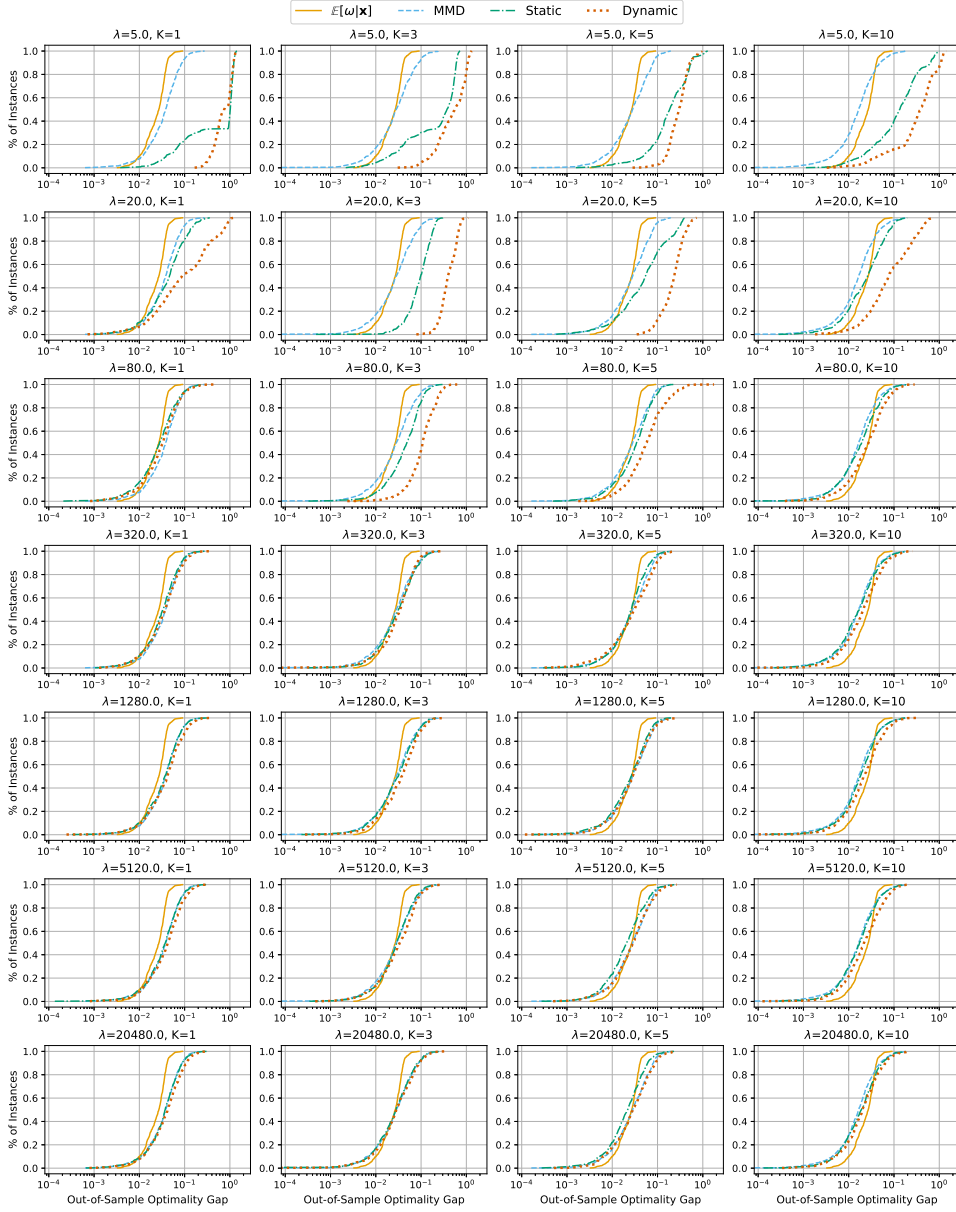
In the case of fashion retail, Vaagen et al. [42] point out that demand is multi-modal with strong dependence. In light of this Narum et al. [20] model demand with a multivariate mixture distribution with binary stochastic variables to determine the regime for the product and two Normal distributions for the specific demand that large or small mean depending on the regime. We reflect these considerations in the contextual setup for the problem, which is as follows.

The context  $\mathbf{x} \in \mathbb{R}^p$  is assumed to be Normally distributed  $N(\mathbf{0}, \Sigma)$  where  $p = 10$  and  $\Sigma_{ij} = \rho^{|i-j|}$  with  $\rho = 0.8$ . We randomly initialize a matrix  $\mathbf{W} \in \mathbb{R}^{m \times p}$  where the elements of  $\mathbf{W}$  come from a standard Normal distribution. The random demand state  $Z \in \{-1, 1\}^m$  is given by  $\text{sign}[\mathbf{W}\mathbf{x} + \boldsymbol{\epsilon}]$ , where  $\boldsymbol{\epsilon} \in \mathbb{R}^m$  represents the idiosyncratic demand uncertainty for each product.  $\boldsymbol{\epsilon}$  is assumed to be multi-variate Normal  $N(\mathbf{0}, \sigma\mathbf{I})$ , where  $\sigma$  is set such that the signal-to-noise ratio is 0.5. Based on product  $i$ 's demand state  $Z_i$ , the demand  $\omega_i$  is distributed according to  $N(\mu_{Z_i}, \sigma_{Z_i}^2)$ . We set  $\mu_{-1} = 5$ ,  $\mu_{+1} = 15$ ,  $\sigma_{-1} = 5/3$ , and  $\sigma_{+1} = 5/2$ . The sampled demand is replaced with 0 if it is negative. To define  $\mathbb{P}_{\omega|\mathbf{x}}$  we sample 80 observations via the aforementioned process.



### C.4.3 MNV Optimality Gap CDFs

Fig. C4 Out of sample optimality gaps for the contextual MNV problem



## C.5 Timing analysis

Tables C1 and C2 show the aforementioned metrics by  $K$ . Results for the newsvendor and CEP1 instances are not shown since directly solving the 2SPs is not as computationally challenging. We focus on the CVaR and MNV problems since the CVaR problem considers 1559 support points to define  $\mathbb{P}_{\omega|\mathbf{x}}$  and MNV is complicated by mixed-binary variables in both stages. We do not show the results by  $\lambda$  as it did not significantly impact timing. Furthermore, we do not show the time to compute solutions via the task nets obtained from static and dynamic approaches since they did not vary relative to the MMD task net (as their architecture is the same).

**Table C1** Computation times (in seconds) for contextual CVaR

$K$	MMD Training	Surrogate Solution Calculation (MMD)	2SP Solve $n_{\text{eval}} = 312$	MMD Loss Evaluation	Loss-Net Training	Static Training	Dynamic Training
1	167.6	1.2	1422.1	13.2	31.5	222.1	766.1
3	172.4	3.0	1465.8	21.9	31.3	219.5	802.1
5	166.7	3.0	1339.4	28.1	30.6	215.9	825.0
10	168.8	5.6	1340.1	46.3	31.7	218.8	935.4
20	167.1	11.1	1331.7	87.4	30.5	214.7	1123.6
40	168.2	33.1	1392.0	273.8	31.5	217.7	1950.2

*Note.* The median over  $\lambda$  is displayed if the relevant method is dependent on  $\lambda$

**Table C2** Median computation times (in seconds) for contextual MNV

$K$	MMD Training	Surrogate Solution Calculation (MMD)	2SP Solve $n_{\text{eval}} = 300$	MMD Loss Evaluation	Loss-Net Training	Static Training	Dynamic Training
1	22.6	0.7	233.0	11.3	20.5	29.5	203.6
3	23.6	2.3	245.3	25.6	21.3	30.4	256.6
5	21.8	4.3	236.1	40.1	18.8	27.5	308.4
10	20.9	8.4	234.1	84.9	19.1	27.9	491.6

## References

- [1] Ntaimo, L.: Example Applications of Stochastic Programming, pp. 111–152. Springer, Cham (2024). [https://doi.org/10.1007/978-3-031-52464-6\\_4](https://doi.org/10.1007/978-3-031-52464-6_4) . [https://doi.org/10.1007/978-3-031-52464-6\\_4](https://doi.org/10.1007/978-3-031-52464-6_4)
- [2] Kleywegt, A.J., Shapiro, A., Homem-de-Mello, T.: The sample average approximation method for stochastic discrete optimization. SIAM Journal on optimization **12**(2), 479–502 (2002) <https://doi.org/10.1137/S1052623499363220>
- [3] Patel, R.M., Dumouchelle, J., Khalil, E., Bodur, M.: Neur2sp: Neural two-stage stochastic programming. Advances in Neural Information Processing Systems **35**, 23992–24005 (2022)

- [4] Wu, Y., Song, W., Cao, Z., Zhang, J.: Learning scenario representation for solving two-stage stochastic integer programs. (2022). International Conference on Learning Representations, ICLR
- [5] Hight, J.L., Sen, S.: Stochastic Decomposition. Kluwer Academic Publishers, Norwell, MA, USA (1996). <https://doi.org/10.1007/978-1-4615-4115-8>
- [6] Sadana, U., Chenreddy, A., Delage, E., Forel, A., Frejinger, E., Vidal, T.: A survey of contextual optimization methods for decision-making under uncertainty. European Journal of Operational Research (2024) <https://doi.org/10.1016/j.ejor.2024.03.020>
- [7] Estes, A.S., Richard, J.-P.P.: Smart predict-then-optimize for two-stage linear programs with side information. INFORMS Journal on Optimization **5**(3), 295–320 (2023) <https://doi.org/10.1287/ijoo.2023.0088>
- [8] Ban, G.-Y., Gallien, J., Mersereau, A.J.: Dynamic procurement of new products with covariate information: The residual tree method. Manufacturing & Service Operations Management **21**(4), 798–815 (2019) <https://doi.org/10.1287/msom.2018.0725>
- [9] Bertsimas, D., Kallus, N.: From predictive to prescriptive analytics. Management Science **66**(3), 1025–1044 (2020) <https://doi.org/10.1287/mnsc.2018.3253>
- [10] Yilmaz, D., Büyüktaktakın, İ.E.: A deep reinforcement learning framework for solving two-stage stochastic programs. Optimization Letters, 1–28 (2023) <https://doi.org/10.1007/s11590-023-02009-5>
- [11] Zharmagambetov, A., Amos, B., Ferber, A., Huang, T., Dilkina, B., Tian, Y.: Landscape surrogate: Learning decision losses for mathematical optimization under partial information. Advances in Neural Information Processing Systems **36** (2024)
- [12] Elmachtoub, A.N., Grigas, P.: Smart “predict, then optimize”. Management Science (2021) <https://doi.org/10.1287/mnsc.2020.3922>
- [13] Agrawal, A., Amos, B., Barratt, S., Boyd, S., Diamond, S., Kolter, J.Z.: Differentiable convex optimization layers. Advances in neural information processing systems **32** (2019)
- [14] Grigas, P., Qi, M., *et al.*: Integrated conditional estimation-optimization. arXiv preprint arXiv:2110.12351 (2021) <https://doi.org/10.48550/arXiv.2110.12351>
- [15] King, A.J., Wallace, S.W.: Modeling with Stochastic Programming. Springer, New York, NY (2012). <https://doi.org/10.1007/978-0-387-87817-1>
- [16] Dupačová, J., Gröwe-Kuska, N., Römis, W.: Scenario reduction in stochastic

- programming. *Mathematical programming* **95**, 493–511 (2003) <https://doi.org/10.1007/s10107-002-0331-0>
- [17] Høyland, K., Kaut, M., Wallace, S.W.: A heuristic for moment-matching scenario generation. *Computational optimization and applications* **24**, 169–185 (2003) <https://doi.org/10.1023/A:1021853807313>
- [18] Bertsimas, D., Mundru, N.: Optimization-based scenario reduction for data-driven two-stage stochastic optimization. *Operations Research* **71**(4), 1343–1361 (2023) <https://doi.org/10.1287/opre.2022.2265>
- [19] Fairbrother, J., Turner, A., Wallace, S.W.: Problem-driven scenario generation: an analytical approach for stochastic programs with tail risk measure. *Mathematical Programming*, 1–42 (2022) <https://doi.org/10.1007/s10107-019-01451-7>
- [20] Narum, B.S., Fairbrother, J., Wallace, S.W.: Problem-based scenario generation by decomposing output distributions. *European Journal of Operational Research* **318**(1), 154–166 (2024) <https://doi.org/10.1016/j.ejor.2024.04.006>
- [21] Lee, J., Bae, S., Kim, W.C., Lee, Y.: Value function gradient learning for large-scale multistage stochastic programming problems. *European Journal of Operational Research* **308**(1), 321–335 (2023) <https://doi.org/10.1016/j.ejor.2022.10.011>
- [22] Bae, H., Lee, J., Kim, W.C., Lee, Y.: Deep value function networks for large-scale multistage stochastic programs. In: *International Conference on Artificial Intelligence and Statistics*, pp. 11267–11287 (2023). PMLR
- [23] Bengio, Y., Frejinger, E., Lodi, A., Patel, R., Sankaranarayanan, S.: A learning-based algorithm to quickly compute good primal solutions for stochastic integer programs. In: *Integration of Constraint Programming, Artificial Intelligence, and Operations Research: 17th International Conference, CPAIOR 2020, Vienna, Austria, September 21–24, 2020, Proceedings 17*, pp. 99–111 (2020). [https://doi.org/10.1007/978-3-030-58942-4\\_7](https://doi.org/10.1007/978-3-030-58942-4_7). Springer
- [24] Römisch, W.: Stability of stochastic programming problems. *Handbooks in operations research and management science* **10**, 483–554 (2003) [https://doi.org/10.1016/S0927-0507\(03\)10008-4](https://doi.org/10.1016/S0927-0507(03)10008-4)
- [25] Gretton, A., Borgwardt, K.M., Rasch, M.J., Schölkopf, B., Smola, A.: A kernel two-sample test. *Journal of Machine Learning Research* **13**(25), 723–773 (2012)
- [26] Muandet, K., Fukumizu, K., Sriperumbudur, B., Schölkopf, B., *et al.*: Kernel mean embedding of distributions: A review and beyond. *Foundations and Trends® in Machine Learning* **10**(1-2), 1–141 (2017) <https://doi.org/10.1561/22000000060>

- [27] Huang, Z., Lam, H., Zhang, H.: Evaluating aleatoric uncertainty via conditional generative models. arXiv preprint arXiv:2206.04287 (2022) <https://doi.org/10.48550/arXiv.2206.04287>
- [28] Sejdinovic, D., Sriperumbudur, B., Gretton, A., Fukumizu, K.: Equivalence of distance-based and rkhs-based statistics in hypothesis testing. *The annals of statistics*, 2263–2291 (2013)
- [29] Séjourné, T., Peyré, G., Vialard, F.-X.: Unbalanced optimal transport, from theory to numerics. *Handbook of Numerical Analysis* **24**, 407–471 (2023) <https://doi.org/10.1016/bs.hna.2022.11.003>
- [30] Székely, G.J., Rizzo, M.L.: On the uniqueness of distance covariance. *Statistics & Probability Letters* **82**(12), 2278–2282 (2012) <https://doi.org/10.1016/j.spl.2012.08.007>
- [31] Wilder, B., Dilkina, B., Tambe, M.: Melding the data-decisions pipeline: Decision-focused learning for combinatorial optimization. In: *Proceedings of the AAAI Conference on Artificial Intelligence*, vol. 33, pp. 1658–1665 (2019). <https://doi.org/10.1609/aaai.v33i01.33011658>
- [32] Sinha, A., Malo, P., Deb, K.: A review on bilevel optimization: From classical to evolutionary approaches and applications. *IEEE transactions on evolutionary computation* **22**(2), 276–295 (2017) <https://doi.org/10.1109/TEVC.2017.2712906>
- [33] Rockafellar, R.T., Wets, R.J.-B.: *Variational Analysis* vol. 317. Springer, Berlin, Heidelberg (2009). <https://doi.org/10.1007/978-3-642-02431-3>
- [34] Zaheer, M., Kottur, S., Ravanbakhsh, S., Póczos, B., Salakhutdinov, R.R., Smola, A.J.: Deep sets. *Advances in neural information processing systems* **30** (2017)
- [35] Tabaghi, P., Wang, Y.: Universal representation of permutation-invariant functions on vectors and tensors. In: *International Conference on Algorithmic Learning Theory*, pp. 1134–1187 (2024). PMLR
- [36] Lin, L.-J.: Self-improving reactive agents based on reinforcement learning, planning and teaching. *Machine learning* **8**, 293–321 (1992) <https://doi.org/10.1007/BF00992699>
- [37] Birge, J.R.: The value of the stochastic solution in stochastic linear programs with fixed recourse. *Mathematical programming* **24**, 314–325 (1982) <https://doi.org/10.1007/BF01585113>
- [38] Liu, C., Letchford, A.N., Svetunkov, I.: Newsvendor problems: An integrated method for estimation and optimisation. *European Journal of Operational Research* **300**(2), 590–601 (2022) <https://doi.org/10.1016/j.ejor.2021.08.013>

- [39] Seabold, Perktold: Statsmodels: Econometric and Statistical Modeling with Python. In: Walt, Millman (eds.) Proceedings of the 9th Python in Science Conference, pp. 92–96 (2010). <https://doi.org/10.25080/Majora-92bf1922-011>
- [40] Koenker, R., Hallock, K.F.: Quantile regression. *Journal of economic perspectives* **15**(4), 143–156 (2001)
- [41] Krokmal, P., Palmquist, J., Uryasev, S.: Portfolio optimization with conditional value-at-risk objective and constraints. *Journal of risk* **4**, 43–68 (2002) <https://doi.org/10.21314/JOR.2002.057>
- [42] Vaagen, H., Wallace, S.W., Kaut, M.: Modelling consumer-directed substitution. *International Journal of Production Economics* **134**(2), 388–397 (2011) <https://doi.org/10.1016/j.ijpe.2009.11.012>
- [43] Pele, O., Werman, M.: Fast and robust earth mover’s distances. In: 2009 IEEE 12th International Conference on Computer Vision, pp. 460–467 (2009). <https://doi.org/10.1109/ICCV.2009.5459199> . IEEE
- [44] Genevay, A., Chizat, L., Bach, F., Cuturi, M., Peyré, G.: Sample complexity of sinkhorn divergences. In: The 22nd International Conference on Artificial Intelligence and Statistics, pp. 1574–1583 (2019). PMLR
- [45] Bellemare, M.G., Danihelka, I., Dabney, W., Mohamed, S., Lakshminarayanan, B., Hoyer, S., Munos, R.: The cramer distance as a solution to biased wasserstein gradients. *arXiv preprint arXiv:1705.10743* (2017) <https://doi.org/10.48550/arXiv.1705.10743>
- [46] Feydy, J., Séjourné, T., Vialard, F.-X., Amari, S.-i., Trounev, A., Peyré, G.: Interpolating between optimal transport and mmd using sinkhorn divergences. In: The 22nd International Conference on Artificial Intelligence and Statistics, pp. 2681–2690 (2019)
- [47] Ren, Y., Zhu, J., Li, J., Luo, Y.: Conditional generative moment-matching networks. *Advances in Neural Information Processing Systems* **29** (2016)
- [48] Park, J., Muandet, K.: A measure-theoretic approach to kernel conditional mean embeddings. *Advances in neural information processing systems* **33**, 21247–21259 (2020)
- [49] Hagemann, P., Hertrich, J., Altekrieger, F., Beinert, R., Chemseddine, J., Steidl, G.: Posterior sampling based on gradient flows of the mmd with negative distance kernel. *arXiv preprint arXiv:2310.03054* (2023) <https://doi.org/10.48550/arXiv.2310.03054>
- [50] Chemseddine, J., Hagemann, P., Wald, C.: Y-diagonal couplings: Approximating posteriors with conditional wasserstein distances. *arXiv preprint*

arXiv:2310.13433 (2023) <https://doi.org/10.48550/arXiv.2310.13433>

- [51] Tietz, M., Fan, T.J., Nouri, D., Bossan, B., skorch Developers: Skorch: A Scikit-learn Compatible Neural Network Library that Wraps PyTorch. (2017). <https://skorch.readthedocs.io/en/stable/>
- [52] Deng, Y., Sen, S.: Predictive stochastic programming. *Computational Management Science*, 1–34 (2022) <https://doi.org/10.1007/s10287-021-00400-0>
- [53] Vaswani, A.: Attention is all you need. *Advances in Neural Information Processing Systems* (2017)